Title
Overview of TFTR transport studies

Journal
Plasma Physics and Controlled Fusion, 33(13)

ISSN
0741-3335

Authors
Hawryluk, RJ
Arunasalam, V
Barnes, CW
et al.

Publication Date
1991-11-01

DOI
10.1088/0741-3335/33/13/005

Plasma Physics and Controlled Fusion, Vol. 33, No. 13, pp. 1509–1536, 1991.
Printed in Great Britain.

0741–3335/91 $3.00 + .00
IOP Publishing Ltd. and Pergamon Press plc.

OVERVIEW OF TFTR TRANSPORT STUDIES

R. J. HAWRYLUK, V. Arunasalam, C. W. Barnes[1], M. Beer, M. Bell, R. Bell, H. Biglari, M. Bitter, R. Boivin, N. L. Bretz, R. Budny, C. E. Bush[2], C. Z. Cheng, T. K. Chu, S. A. Cohen, S. Cowley, P. C. Efthimion, R. J. Fonck[3], E. Fredrickson, H. P. Furth, R. J. Goldston, G. Greene, B. Grek, L. R. Grisham, G. Hammett, W. Heidbrink[4], K. W. Hill, J. Hosea, R. A. Hulse, H. Hsuan, A. Janos, D. Jassby, F. C. Jobes, D. W. Johnson, L. C. Johnson, J. Kesner[5], C. Kieras-Phillips, S. J. Kilpatrick, H. Kugel, P. H. La Marche, B. LeBlanc, D. M. Manos, D. K. Mansfield, E. S. Marmar[5], E. Mazzucato, M. P. McCarthy, M. Mauel[6], D. C. McCune, K. M. McGuire, D. M. Meade, S. S. Medley, D. R. Mikkelsen, D. Monticello, R. Motley, D. Mueller, Y. Nagayama[7], G. A. Navratil[6], R. Nazikian, D. K. Owens, H. Park, W. Park, S. Paul, F. Perkins, S. Pitcher[8], A. T. Ramsey, M. H. Redi, G. Rewoldt, D. Roberts[3], A. L. Roquemore, P. H. Rutherford, S. Sabbagh[6], G. Schilling, J. Schivell, G. L. Schmidt, S. D. Scott, J. Snipes[5], J. Stevens, B. C. Stratton, W. Stodiek, E. Synakowski, Y. Takase[5], W. Tang, G. Taylor, J. Terry[5], J. R. Timberlake, H. H. Towner, M. Ulrickson, S. von Goeler, R. Wieland, M. Williams, J. R. Wilson, K. L. Wong, M. Yamada, S. Yoshikawa, K. M. Young, M. C. Zarnstorff, and S. J. Zweben

Plasma Physics Laboratory, Princeton University
P.O. Box 451 Princeton, New Jersey 08543 USA

[1]Los Alamos National Laboratory, New Mexico
[2]Oak Ridge National Laboratory, Oak Ridge, TN
[3]University of Wisconsin, Madison, WI
[4]University of California, Irvine, CA
[5]Massachusetts Institute of Technology, Cambridge, MA
[6]Columbia University, New York, NY
[7]University of Tokyo, Tokyo, Japan
[8]Canadian Fusion Fuels Technology Project, Toronto, Canada

ABSTRACT

A review of TFTR plasma transport studies is presented. Parallel transport and the confinement of suprathermal ions are found to be relatively well described by theory. Cross-field transport of the thermal plasma, however, is anomalous with the momentum diffusivity being comparable to the ion thermal diffusivity and larger than the electron thermal diffusivity in neutral beam heated discharges. Perturbative experiments have studied non-linear dependencies in the transport coefficients and examined the role of possible non-local phenomena. The underlying turbulence has been studied using microwave scattering, beam emission spectroscopy and microwave reflectometry over a much broader range in $k_\perp$ than previously possible. Results indicate the existence of large-wavelength fluctuations correlated with enhanced transport.

MHD instabilities set important operational constraints. However, by modifying the current profile using current ramp-down techniques, it has been possible to extend the operating regime to higher values of both $\varepsilon\beta_p$ and normalized β_T. In addition, the interaction of MHD fluctuations with fast ions, of potential relevance to α-particle confinement in D-T plasmas, has been investigated. The installation of carbon-carbon composite tiles and improvements in wall conditioning, in particular the use of Li pellet injection to reduce the carbon recycling, continue to be important in the improvement of plasma performance.

I. INTRODUCTION

Transport studies have been a principal focus of the research activities on TFTR for two main reasons. First, in order to achieve TFTR's research objectives during the D-T phase, a regime of enhanced confinement ("supershots") compared with L-mode has had to be developed to enhance the plasma reactivity (Strachan *et al.*, 1987; Hawryluk *et al.*, 1987; Bell *et al.*, 1988; and Meade *et al.*, 1990) Second, results from transport studies have important implications for the design and eventual operation of the next generation of devices (BPX and ITER). During the past three years, transport studies have been given renewed emphasis in the U.S. program with the establishment of a national Transport Task Force (TTF) (Callen *et al.*, 1990). Comprehensive reviews of transport issues have been recently published by the TTF (Boozer *et al.*, 1990; Wootton *et al.*, 1990; Burrell *et al.*, 1990; Houlberg *et al.*, 1990; Kaye *et al.*, 1990; and Stambaugh *et al.*, 1990). On TFTR, detailed transport studies have been performed in a broad range of operating conditions (ohmic, L-mode, supershot, pellet enhanced, and H-mode) to characterize and understand the transport mechanisms with the goal of improving plasma performance. As will be discussed below, these experiments have supported the predictions of some theoretical models. However, in other areas, some of the underlying assumptions commonly used have been brought into question. This paper will provide a summary of the principal transport studies conducted on TFTR and will highlight those experimental results which a comprehensive theory of plasma transport would have to describe.

This paper will begin by reviewing parallel transport and the confinement of suprathermal ions, both of which are relatively well described by theory. The more complex topic of cross-field transport of the thermal components will then be discussed. Perturbative experiments will be described which test various theoretical models and address the role of non-linear or non-local mechanisms. In addition, studies of confinement scaling in terms of non-dimensional parameters have been conducted to form a physics-based approach to predict the performance of future machines. Studies of the underlying turbulence and the role of MHD instabilities on transport and confinement will be summarized. The paper will conclude with a brief discussion of the development of wall conditioning techniques, which continue to play a key role in plasma confinement experiments.

A description of the machine hardware capabilities for the experiments described here has been given by Meade *et al.* (1990). TFTR has a circular cross-section plasma with minor radius, a, variable from 0.4m to 0.96m and major radius, R_p, variable from 2.1m to 3.1m. The toroidal field system is operated at the full field rating of B_T = 5.2T and plasma currents I_p up to 3MA have been achieved. The neutral beam system has injected a total power of up to P_{NBI} = 33MW. The ICH systems have coupled into the plasma up to P_{ICH} = 6.3MW. The limiter system for TFTR consists of an axisymmetric inner-wall bumper limiter and two carbon/carbon composite poloidal rings on the outer cross-section to protect the ICH antennas. In early 1990, the graphite tiles in the high heat flux regions of the inner-wall bumper limiter were replaced with carbon-carbon fiber reinforced tiles. TFTR has two pellet injectors. An eight barrel D_2 pellet injector, developed and built by Oak Ridge National Laboratory, produces pellets of 3, 3.5 and 4 mm diameter at speeds of ~1.5km/sec. A two barrel lithium or carbon pellet injector developed, built and operated by Massachusetts Institute of Technology, produces 2mm pellets at 0.8km/sec for fueling, diagnostic, and wall coating experiments.

The experiments which will be described principally involve auxiliary heated discharges in the supershot, L-mode and H-mode regimes. Plasma parameters extend up to $T_i(0)$ = 35keV, $T_e(0)$ = 12keV, $n_e(0) \approx 1.2 \times 10^{20}\,m^{-3}$ producing D-D neutron rates up to 5×10^{16}/sec in supershots. The fusion parameter $n_e(0)\tau_E T_i(0)$ in supershot plasmas has reached values of $4.4 \times 10^{20}\,m^{-3}\cdot sec\cdot keV$. Hot-ion plasmas combining peaked density profiles with the edge characteristics of H-mode plasmas have been produced in circular cross-section discharges yielding $n_e(0)\tau_E T_i(0)$ values characteristic of supershots (Bush *et al.*, 1990). With deuterium-pellet injection, central densities of $5 \times 10^{20}\,m^{-3}$ have been achieved enabling the study of high density discharges as well.

II. PARALLEL TRANSPORT

The plasma response to the inductive electric field and other sources of current is analyzed using the neoclassical (classical Spitzer resistivity plus trapped-particle effects) Ohm's law obtained from parallel electron momentum balance (Hirshman and Sigmar, 1981). On TFTR, Zarnstorff *et al.* (1990a) found the plasma surface voltage in ohmically-heated discharges to be in good agreement with the predictions of neoclassical resistivity and in disagreement with the predictions of classical resistivity when the measured temperature profile, Z_{eff}, equilibrium parameters and the calculated bootstrap current ($\leq 5\%$ of I_p) were taken into account. This agreement is in contrast with the observed cross-field electron transport which is typically much larger (>100) than neoclassical predictions. In these experiments, the collision frequency ν_e^* ($r = a/2$) was varied from 0.07 to 2, enabling a detailed test to be made of the predictions of the neoclassical resistivity over the transition from the banana into the plateau regime.

During moderate current ramps ($dI_p/dt \leq 1MA/s$) both the surface voltage and the location of the q = 1 surface are well predicted on the basis of neoclassical resistivity. Fredrickson *et al.* (1987) performed current penetration studies with higher current ramping rates, up to 3.2MA/s. In these cases, bursts of MHD activity were observed during the ramp as q(a) crossed rational values of 5, 4.5 and 4. A small disruption was observed at the q(a) = 4 crossing which was accompanied by a drop in the electron temperature. The resulting increase in the calculated resistivity due to the rapid change in the electron temperature enhanced the calculated current penetration, and resulted in good agreement with the experiment without having to postulate anomalous current diffusion. Current diffusion has not been studied during the initial 200ms of the discharge, when the current ramp rate is faster ($dI_p/dt \geq 5MA/s$).

Currents driven by density and temperature gradients (bootstrap current) and by unthermalized beam ions due to unbalanced (co- and counter-tangential) injection are also well predicted by neoclassical theory. These have been extensively studied by Zarnstorff *et al.* (1987, 1988a) and Scott *et al.* (1989) who found good agreement with neoclassical predictions using the time-dependent analysis code TRANSP (Hawryluk, 1980; Goldston *et al.*, 1981). In Fig. 1, the measured surface voltages in two discharges are compared with predictions of neoclassical theory for nearly balanced injection (Fig. 1a) in which the bootstrap current is predicted to be dominant (up to 65%), and with co-injected neutral beams only (Fig. 1b) in which the beam-driven current dominates. In evaluating the co- only injection discharge, it was necessary to include the effects of the measured toroidal plasma rotation on beam deposition and slowing-down of the beam ions to obtain agreement. The agreement with theory in these experiments has given strong support to the models presently used to calculate the bootstrap and the beam driven current in future devices such as BPX and ITER.

III. FAST ION CONFINEMENT

Cross-field transport of fast ions (beam injected ions, multi-MeV fusion products and minority ions heated by ICH) comparable to that for the thermal plasma would have substantial implications not only for the interpretation of present experiments but also for reactor requirements. This topic has been extensively studied on TFTR. An elegant experiment by Radeztsky *et al.* (1988), using tangential neutral beams injected into the edge of a discharge and a tangentially viewing detector to measure the charge-exchange neutral flux, placed an upper bound on the diffusivity of passing fast ions (30-90keV) of $D_{fast} < 0.05m^2/s$. Recently, short (~20ms) pulses of injected beam ions were used to study the confinement of both passing and trapped

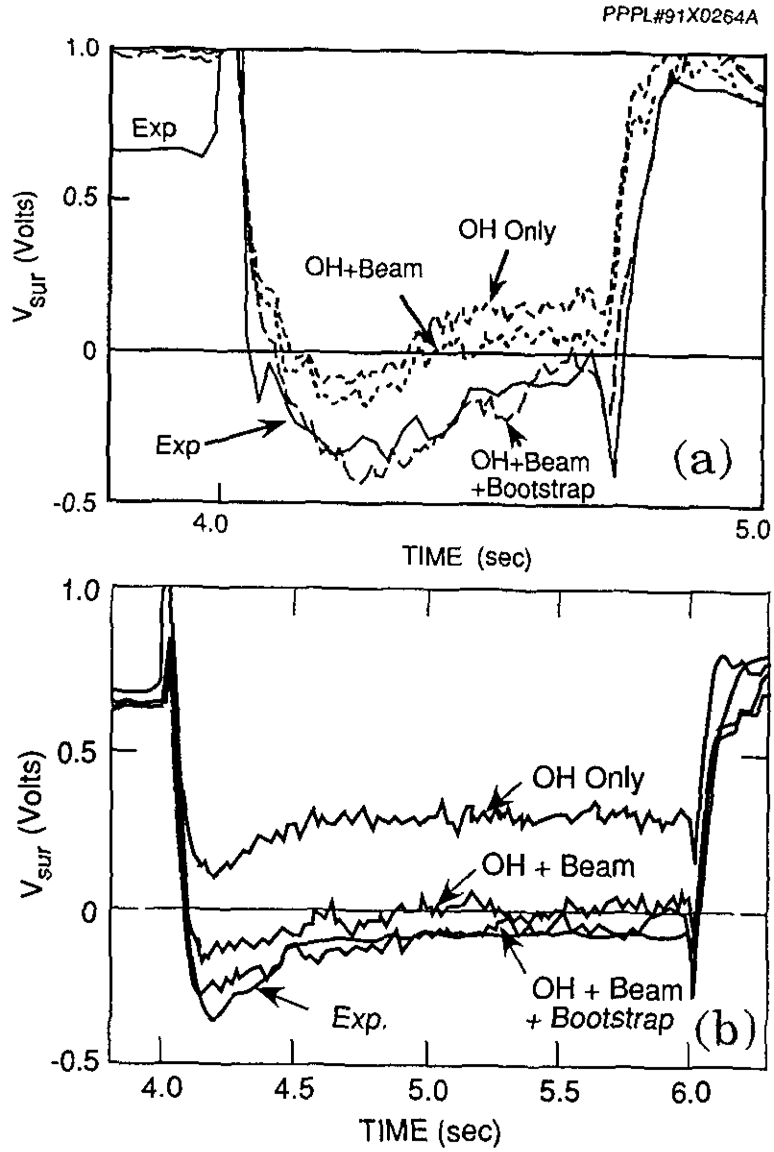

Fig. 1 a) The measured surface voltage in a discharge with nearly balanced injection compared with TRANSP simulations including driven currents and with simulations excluding the bootstrap current and without the beam-driven current. (I_p = 1.0MA, P_{NBI} = 11MW)
b) Same comparison for a discharge heated by co-injection. (I_p = 1.0MA, P_{NBI} = 11MW, V_ϕ = 8 x 10^5m/s)

particles (90keV) (Scott *et al.*, 1990; Heidbrink *et al.*, 1991). The decay rate of the fusion neutron production following the pulse was found to agree well with theoretical calculations based on classical slowing down and no radial diffusion. An upper bound on the radial transport was inferred to be $0.1 m^2/s$. This conclusion was also supported by measurements of the neutron emission profile and measurements of charge-exchange neutrals along two vertically viewing chords.

Measurements of the ICH-generated energetic ions in TFTR indicate that these trapped ions experience very little radial transport compared to the strong anomalous transport of the thermal plasma. Figure 2 shows the measured flux of 100keV hydrogen to a charge-exchange detector viewing vertically through the plasma at a major radius of 3.23m (= $R_p + 0.65a$, with $R_p = 2.61m$ and $a = 0.96m$ for this plasma), as a function of the cyclotron resonance layer position. Since the detector is viewing perpendicular to the magnetic field, it sees particles which have charge-exchanged at their banana tips. The ICH accelerates the hydrogen primarily in $v_\perp$, thus producing a very large signal when the resonance layer is directly over the detector. Figure 2 presents the predicted flux (normalized at R = 3.2m) from a comprehensive bounce-averaged quasilinear Fokker-Planck code (Hammett, 1986). This code is coupled to a full-wave ICH deposition code (Smithe *et al.*, 1987) which calculates the propagation and deposition of the fast wave. The measurements can be matched with $D_{fast} = 0.05 m^2/s$, which is larger than the neoclassical prediction, $\sim 0.01 m^2/s$, but roughly consistent with the transport expected to be caused by toroidal field ripple. Nevertheless, the fast ions experience very little cross-field transport relative to the electron thermal diffusivity, χ_e, which was $1 m^2/s$.

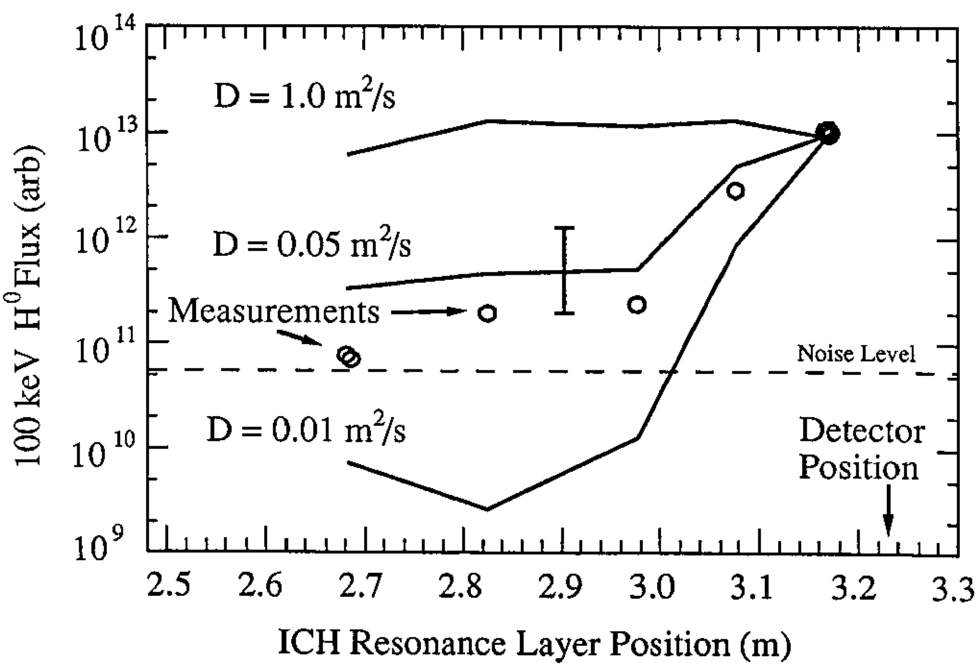

Fig. 2 Charge-exchange measurements of 100keV resonant minority ions as a function of the location of the ICH resonance layer compared with the results of Fokker-Planck calculations for different levels of radial transport.

Fast tritons produced by d(d,p)t reactions at 1MeV, which slow down primarily by electron drag, may undergo subsequent t(d,n)α reactions to produce 14MeV neutrons. *The triton burnup fraction (in steady-state,* the ratio of the D-T neutron to the D-D neutron rate) is a very sensitive function of triton slowing down and confinement. The ratio of the measured triton burnup fraction to the expected fraction is less than one and tends to decrease (to about 0.3) in discharges with long slowing-down times (Scott *et al.*, 1990c). The discrepancy is consistent with a radial diffusion coefficient of ~$0.1 m^2/s$. Radial diffusion of fast fusion products at this rate in the burning plasmas of BPX or ITER would not be a severe loss, due to the relatively short thermalization times for fusion alpha particles.

Direct measurements of the loss of MeV D-D fusion products (tritons and protons) near the bottom of the vacuum vessel wall (45°-90° below the outer midplane) and just below the midplane are shown in Figs. 3 and 4. The loss of fusion products away from the midplane is consistent with the expected first-orbit loss in MHD quiescent discharges and is observed to decrease with increasing current (Zweben *et al.*, 1990). (The effects of MHD on fast particle behavior will be discussed in Sec. VIII). The cross-field diffusivity of passing particles above 0.5MeV has been shown to be $D_{fast} \lesssim 0.1 m^2/s$ (Zweben *et al.*, 1991). A midplane probe has been used to study loss associated with toroidal field stochastic ripple diffusion (Boivin

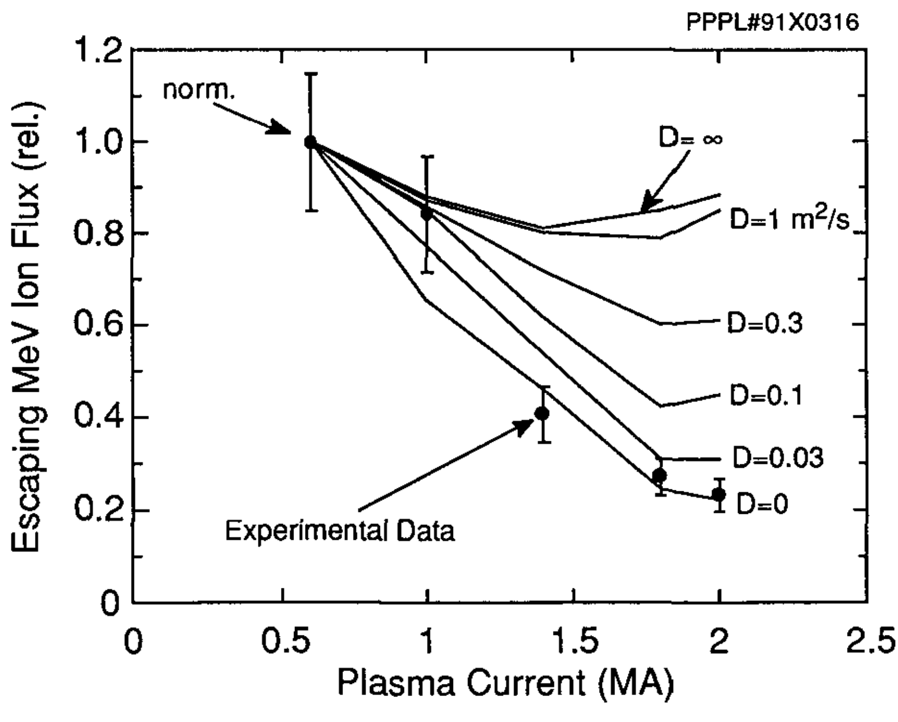

Fig. 3 Ratio of the measured ion loss to the total neutron flux versus plasma current for a probe mounted at the bottom of the vessel. The calculated curves include losses due to bad orbits and increasing levels of the radial diffusivity. The observed decrease in ion loss with plasma current is consistent with the predicted loss of ions on bad orbits only, indicating little cross-field transport. (R_p = 2.60m, B_T = 3.7T, P_{NBI} = 5 - 12MW)

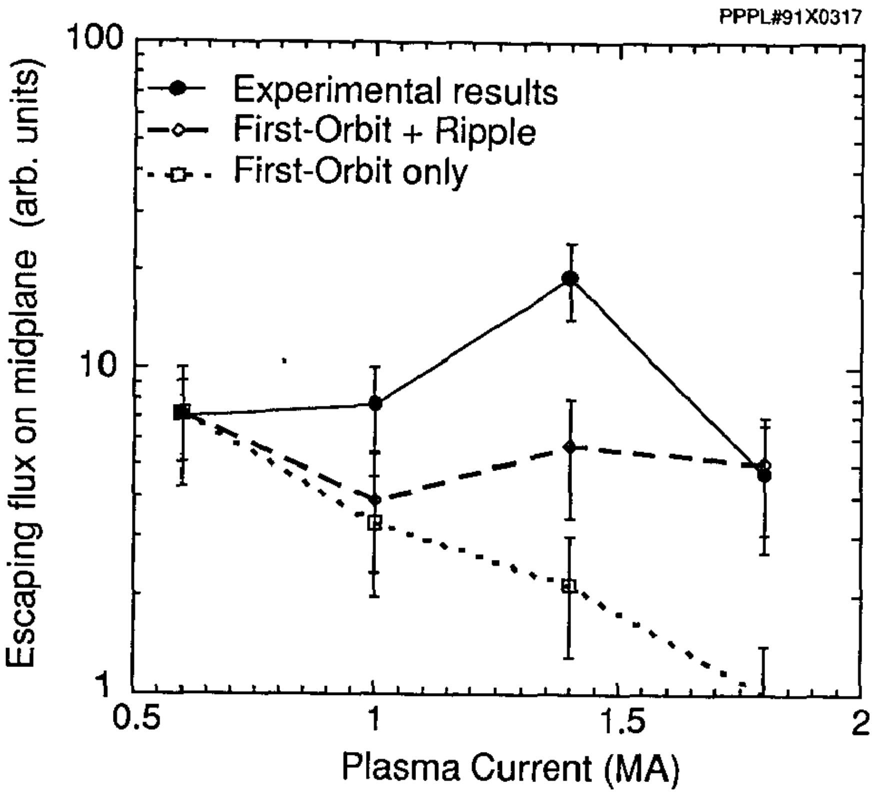

Fig. 4 Ratio of the measured ion loss to the total neutron flux versus plasma current for a probe mounted near the midplane for the same scan shown in Fig. 3. The predicted losses due to bad orbits and toroidal field ripple stochastic diffusion are shown.

et al., 1991). This is a potentially important transport mechanism because, when the ripple strength exceeds about 0.1%, the bounce point of the energetic ion diffuses vertically until the ion hits the wall. Initial modeling of the TF ripple diffusion and the experimental measurements are in reasonable accord, as shown in Fig. 4 for the same data set as in Fig. 3, confirming the presence of the losses predicted by Goldston, White, and Boozer (1981). The difference between the model and the experimental results is believed to be due to the location of the detector, which is placed outside the RF limiter radius, but well inside the first wall. The detector can sample part of the confined ion population, explaining qualitatively the additional flux at medium currents.

The lack of strong anomalous transport for the fast ions, as found in all of these measurements, is believed to be the result of two effects. The dominant reason is that, in the absence of high-frequency MHD, e.g., Alfvénic fluctuations such as the toroidal Alfvén eigenmode (TAE) or kinetic ballooning modes, there are no resonant modes for the fast ions in these experiments (Efthimion *et al.*, 1989; Biglari and Chen, 1991). This favorable circumstance may not be satisfied in the D-T phase of TFTR operation, where α-particles are expected to destabilize both TAE and kinetic ballooning modes, as will be discussed in Sec. VIII. A secondary factor is that even if the resonance condition could be satisfied, orbit-averaging effects, which occur when the ion banana width is large compared to the turbulence correlation length, reduce the driving force (Mynick and Duvall, 1989).

IV. CROSS-FIELD TRANSPORT

Cross-field transport studies have been conducted over a large parameter range ($0.3 < I_p < 3$MA, $1 < B_T < 5$T, $0.4 < a < 0.9$m, $2.1 < R_p < 3.1$m, $P_{NBI} \leq 33$MW, and $P_{ICH} \leq 6.3$MW) and in many operating regimes (L-mode, supershot, H-mode, and with pellet injection). Furthermore, a sophisticated set of profile diagnostics with good spatial and temporal resolution has enabled us to conduct perturbation experiments to test various theoretical models.

The results from the steady-state transport studies, which have been described in detail by Scott *et al.* (1989, 1990a-c), Zarnstorff *et al.* (1989a,b) and Efthimion *et al.* (1991b), will be briefly summarized. The effective ion heat diffusivity, $\chi_i^{eff} \equiv -q_i/n_i\nabla T_i$, is large compared with the neoclassical value (Fonck *et al.*, 1989), a result similar to the DIII observations by Groebner *et al.* (1985). The electron, χ_e^{eff}, and momentum χ_ϕ^{eff} diffusivities are also much larger than neoclassical. In general, $\chi_\phi^{eff} \approx \chi_i^{eff} > \chi_e^{eff}$ *in both the supershot regime, in which* the density profile is highly peaked on axis, and in the L-mode regime with broad density profiles. This is shown in Fig. 5. As the density profile peakedness $n_e(0)/\langle n_e\rangle$ is varied from 1.5 to 3 largely by changes in wall recycling, the resulting discharge conditions vary continuously from the L-mode to the supershot *regime with variations of* τ_E/τ_E^L from 1 to 3, where τ_E^L is the prediction of L-mode scaling (Goldston, 1984). During this process, χ_i^{eff} is reduced by a factor up to eight within $r < a/2$ whereas χ_e^{eff} is reduced by a factor of only about two. The particle diffusivity (ignoring possible pinches) is of the same order as χ_e^{eff} in the plasma core $\chi_e^{eff} \approx (2 - 2.5) \times D^{eff}$ at $r/a \approx 0.27$ and decreases as the density *profile peakedness increases.* In the core of high current supershot discharges, both χ_i^{eff} and χ_e^{eff} decrease with increasing neutral beam power despite the fact that the usual driving terms (T_i, T_e, n_e, β....) all increase.

Ion energy transport becomes so low in the core of supershot plasmas that heat conduction is negligible compared to convection. This contrasts with the usual situation in L-mode discharges where conduction dominates. The strong central fueling by the beam particles provides a well defined source of particles and heat, which in steady-state is balanced by an outward flux. The ratios $Q_e/\Gamma_e T_e$ and $Q_i/\Gamma_i T_i$ (where Q and Γ are the respective heat and particle fluxes) yield upper bounds on the minimum value of the ratio of heat transport by convection to particle flux for each species (Zarnstorff et al., 1988b; 1989a). It is found that in supershots, the upper bound on the minimum value of $Q_i/\Gamma_i T_i$ is ~3/2 for balanced and counter-beam injection, though for highly-rotating plasmas with co-only injection the upper bound is ≤ 1. The upper bound on the minimum value of $Q_e/\Gamma_e T_e$ is typically ~2 independent of the direction of beam injection. The values of these upper bound ratios are found to increase with minor radius, corresponding to an increase of conduction compared with convection, assuming that the multiplier on the convection term does not change with minor radius. Comparing the measured ratio of $Q(r)/\Gamma(r)T(r)$ with theory appears to be a promising technique for evaluating different models of anomalous transport.

The relationships between χ_e^{eff}, χ_i^{eff}, χ_ϕ^{eff} and the particle diffusivities, as well as the upper bound on the convective heat flux, place significant constraints on theoretical transport models. The observation that $\chi_e^{eff} < \chi_i^{eff} \sim \chi_\phi^{eff}$ is consistent with the predictions for electrostatically-driven transport. It is inconsistent with $V_\parallel B$ transport being the predominant mechanism throughout the plasma, although an electromagnetic model in which the turbulence is intermittent or the

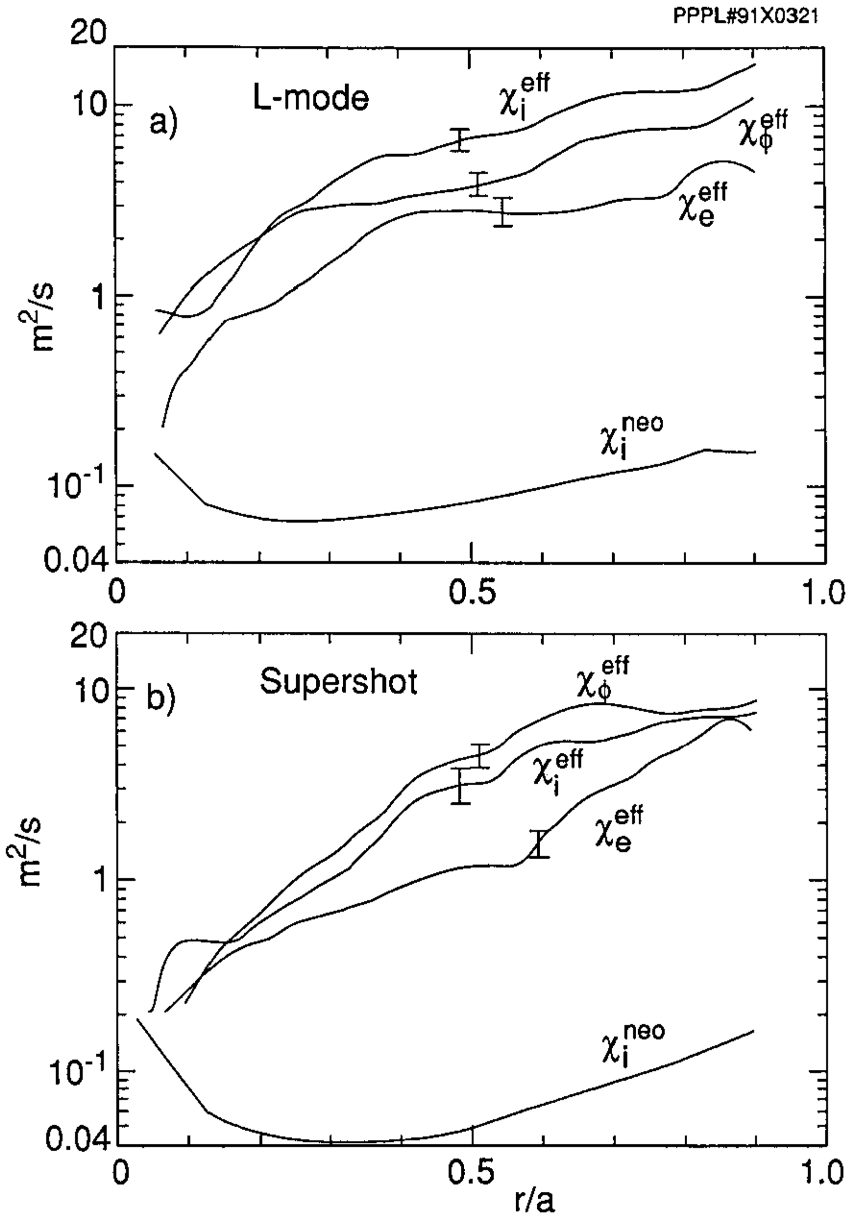

Fig. 5 Variations of χ_e^{eff}, χ_i^{eff} and χ_ϕ^{eff} and χ_i^{neo} with minor radius for a) an L-mode plasma and b) a supershot. For both discharges $R_p = 2.45m$, $a = 0.8m$, $I_p = 1.3MA$, $P_{NBI} = 21MW$.

transport along stochastic field lines occurs in some regions where the surfaces are destroyed, while other intact regions provide an effective transport barrier, may still be possible. However, for models in which transport along stochastic magnetic fields determine the transport, the minimum ratio of $Q_e/\Gamma_e T_e$ should be of order $\sqrt{m_i/m_e}$ whereas for the electrostatic driven transport $Q_e/\Gamma_e T_e \sim 1.5$. Once again the data suggests that electrostatic turbulence is dominant, at least in the case of supershots.

Analysis of momentum transport avoids some of the complications associated with the analysis of heat transport because the convective momentum loss is much less important and the inertia of electrons is not significant. In addition, it provides further insight into another important plasma property. The central rotation speed during neutral beam heating modulated at 5Hz (Scott *et al.*, 1987) showed a clear modulation with centrally-weighted heating. During modulated edge-weighted heating, in which the beam deposition profile peaked at r/a = 0.6, the central rotation velocity showed a simple secular rise. This behavior is consistent with a simple diffusive momentum transport mechanism (without a momentum pinch) with a χ_ϕ^{eff} that *is a factor of ~2 higher during central heating than during edge heating.* The observation that the final rotation speed attained after 3 beam cycles of edge-heating was fully 2/3 of that attained during central-heating implies that diffusive transport of momentum must dominate in this experiment over all local momentum damping mechanisms (e.g. ripple, charge-exchange) as well as any outwardly directed momentum flows (i.e. a positive pinch velocity).

The diffusive nature of momentum transport is also apparent in the evolution of the velocity profile $v_\phi(R)$ from an edge-peaked to a flat profile during the first 500ms of constant edge heating as shown in Fig. 6 (Takase, *et al.*, 1991). Similar to the modulated-beam data, the measured velocity profile can be reproduced without introducing a momentum pinch. Interestingly, the velocity profile "fills in" from the edge in an apparently diffusive manner, while the inferred (neoclassical) electrostatic potential increases secularly with time, due to the increasing velocity. This indicates that momentum transport cannot be driven by a relaxation of the electrostatic potential, as would be expected for example from ripple or electromagnetic turbulence coupled to the wall. Similarly, we observe no changes in local temperatures and no changes in local heat-transport coefficients in rotating or quasi-stationary L-mode plasmas if the rotation speed is perturbed by transiently altering the mix of co- and counter-injecting beams (at constant P_{NBI}).

The variation of τ_E with aspect ratio ($2.8 < R/a < 8.0$) has been studied by Grisham *et al.* (1990, 1991) in L-mode plasmas. The confinement time deduced from the diamagnetic measurement is in reasonable agreement with the ITER power scaling relationship (Yushmanov *et al.*, 1990) multiplied by a factor 0.8 - 0.85. However, the confinement deduced from detailed kinetic *profile measurements yields a more* favorable dependence on aspect ratio, $\tau_E \propto R^{(1.7 - 1.8)} a^0$, closer to the scaling of Goldston (1984). In this experiment, an especially interesting observation is that χ^{eff} is better described as a function of the local inverse aspect ratio ($\varepsilon = r/R$) than as a function of normalized minor radius (r/a). This data suggests that increasing inverse aspect ratio, rather than the local value of electron temperature or q, is responsible for the enhanced transport in the plasma periphery. The isotope dependence of cross-field transport was also studied in a series of ohmic and L-mode NBI discharges. The scaling of energy confinement with ion mass is found to be weaker than expected: for TFTR $\tau_E \propto A^{0.24}$ whereas for ITER-P $\tau_E \propto A^{0.5}$. Due to the difficulty in changing from deuterium to hydrogen in TFTR, there was a significant concentration (25 - 55%) of deuterium in the nominally hydrogen discharges that has been taken into account in deriving the exponent for the mass.

V. PERTURBATION EXPERIMENTS

The radial variation of particle and heat fluxes (and the resulting variation of the density and temperature profiles) has been explored in a series of perturbation experiments. Electron particle and thermal transport coefficients were measured during a controlled scan in which the plasma temperature was varied by a factor of 2 while the electron density, plasma current, and toroidal magnetic field were held constant (Efthimion *et al.*, 1991a). The purpose was to determine if there is any

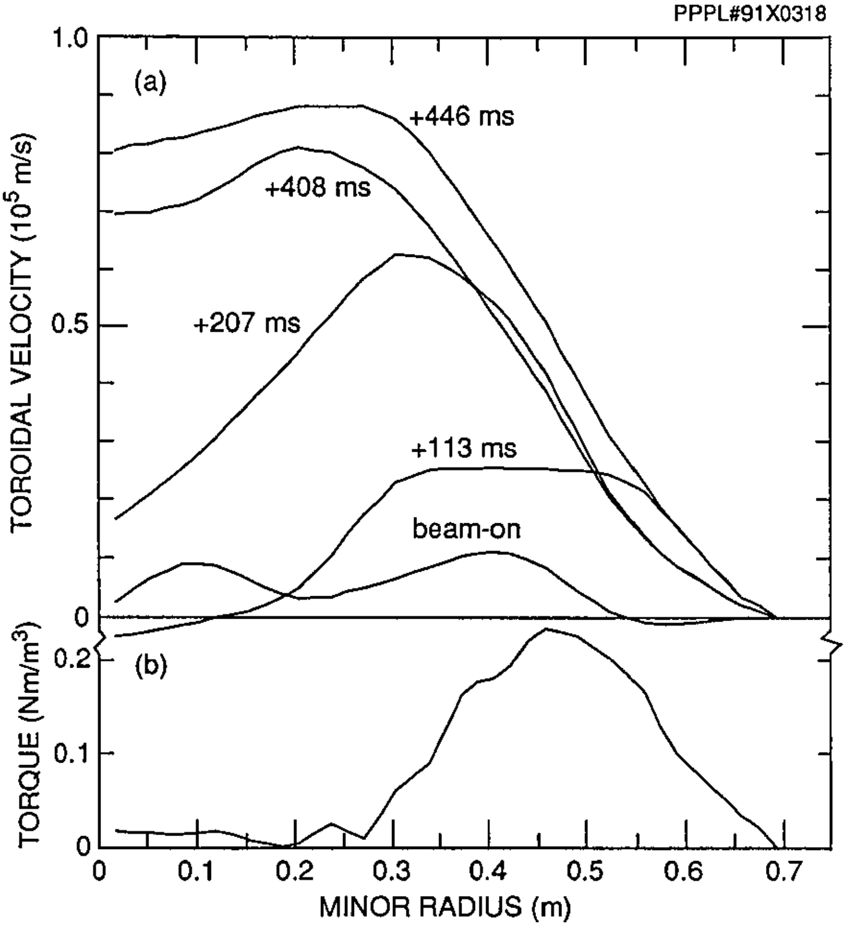

Fig. 6 Profiles of a) the toroidal rotation velocity at increasing times through the beam pulse and b) the toroidal torque from the injected neutral beam during an edge-heating experiment. (R_p = 2.3m, B_T = 5T, I_p = 1.2MA, P_{NBI} = 1.1MW)

explicit temperature dependence of electron transport in auxiliary heated plasmas. The particle transport was measured with a perturbative gas puffing technique. A small amount of gas is introduced at the edge during a steady-state beam-heated plasma and the time evolutions of the density profile and the particle sources are used to ascertain the particle transport coefficients. The analysis uses a general flux relationship that allows for nonlinear transport which is fitted to the experimental particle flux over the time of the perturbation at each plasma radius: $\delta\Gamma = (\partial\Gamma/\partial\nabla n)\delta\nabla n + (\partial\Gamma/\partial n)\delta n$ where the transport coefficients are in terms of these partial derivatives. Previously, Efthimion *et al.* (1989) analyzed the perturbed flux with the assumption that $\Gamma = -D\nabla n + \mathbf{v}n$ which inherently assumed that D and the pinch velocity $\mathbf{v}$ are weak functions of n and ∇n. This assumption has been found to be incorrect. In the temperature scan, the electron thermal diffusivity profile, $\chi_e^{eff}(r)$, was obtained from equilibrium power balance analysis. The analysis of the particle and heat transport coefficients yields local temperature dependencies varying as T_e^{α} where α = 1.5 – 2.5. Quasilinear models of microinstability theory have predicted this observed temperature dependence (Rewoldt and Tang, 1990) for the toroidal drift mode destabilized by the combined influence of trapped electrons and ion temperature gradients. It should be noted that $\chi^{eff} \propto T^{1.5}$ would result in $\tau_E \sim P_{NBI}^{-0.6}$ which is approximately consistent with the widely observed L-mode confinement power scaling.

Taking the partial derivatives of the particle fluxes $\partial\Gamma/\partial\nabla n$ and $\partial\Gamma/\partial n$ at each radius one can look for additional dependencies in the data. The two partial derivatives normalized to the temperature dependence vary with minor radius by factors of 30 to 50. There are few parameters that can fit the radial variations, and comply with the constraint $\partial/\partial n(\partial\Gamma/\partial\nabla n) = \partial/\partial\nabla n(\partial\Gamma/\partial n)$. The parameters that do satisfy the cross-partial constraint and the large variation in the normalized partial derivatives are the density and temperature scale lengths. The functional fits to the partial derivatives are integrated to obtain the form of the total particle flux. The best fits to the data are fluxes of the form $(\varepsilon T_e^{(1.5-2.5)}/n_e L_n^2)\nabla n$, and $(\varepsilon T_e^{(1.5-2.5)}/n_e L_n L_{Te})\nabla n$ in addition to a pinch term on the order of the neoclassical value. The strong scale-length dependence can be

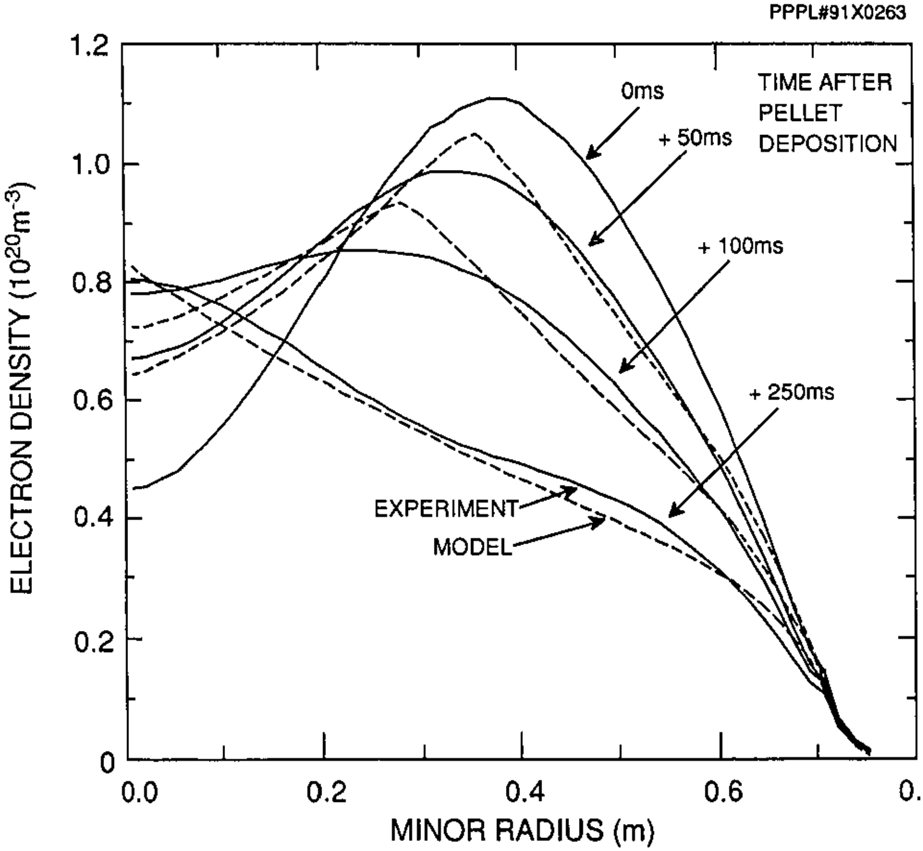

Fig. 7 The evolution of the measured density profile after pellet injection compared with modelling assuming D = $2.4 \times 10^{19}(r/R)(T_e^2/n_e L_n^2)$ and the neoclassical pinch.

reduced if the local q is included in the expressions. These expressions are consistent with electrostatic turbulent transport models (Ross *et al.*, 1987).

Whether the highly nonlinear dependence of the particle flux on density scale length and other terms indicated by the gas puff perturbation experiments is consistent with the density profile response to much larger amplitude perturbations has been studied using the relaxation of density profiles following deuterium pellet injection (Hulse *et al.*, 1991). A beam-heated plasma fueled by six pellets presented a wide range of density scale lengths, including evolution from strongly hollow to strongly peaked profiles with a central density up to ~10 times that in the gas puff experiments. As shown in Fig. 7, the evolution of the density profile following one of the pellets is reasonably well predicted using a transport model with the same functional form as that derived from the gas puff analysis. While the present level of agreement does not provide proof that this particular transport model is uniquely correct, it does provide encouragement that highly nonlinear models consistent with theoretical expectations for electrostatic turbulent transport can be used to interpret and model density transport over a substantial range of plasma conditions. However, in the core of supershot discharges, this particular model overestimates the observed fluxes.

A related transport issue of considerable importance to ITER is the transport of trace impurities, in particular helium and iron. Charge-exchange recombination spectroscopy (Synakowski *et al.*, 1990; Stratton, *et al.*, 1991) has been used to measure the evolution of the helium and helium-like iron profiles after either the injection of a short gas puff or the injection of iron using the laser-blow-off technique. There are important differences between the behavior of the electron

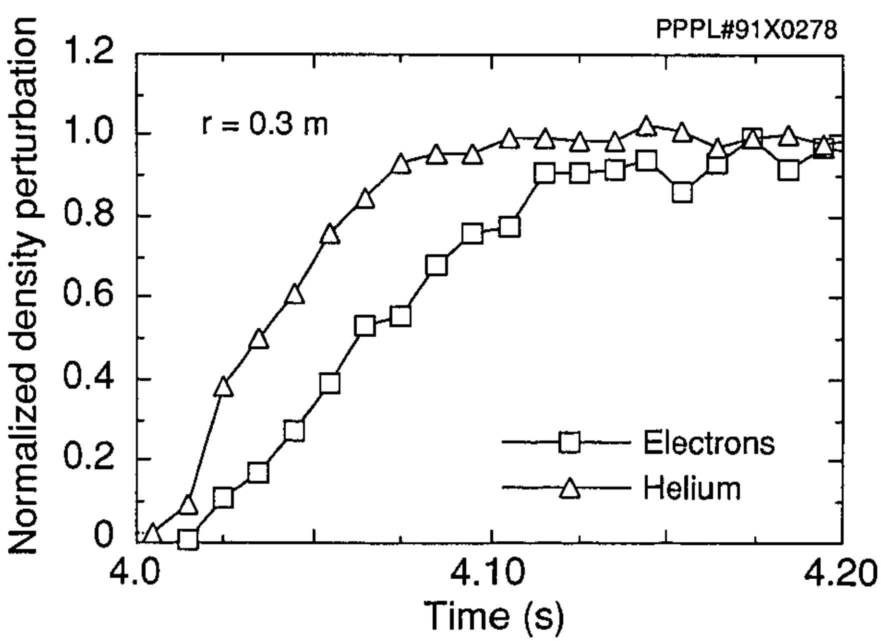

Fig. 8 Evolution of the perturbed electron density and helium density normalized to their final levels at r/a = 0.38 following a short He gas puff into a series of similar L-mode plasmas (R_p = 2.45m, I_p = 1.0MA, P_{NBI} = 13MW).

perturbation and impurities. As shown in Fig. 8, the helium density and the perturbed electron density are found to have a different temporal behavior suggesting that the background ions (deuterium and carbon) are responding to achieve charge neutrality. In addition, as shown in Fig. 9, the helium profile in the supershot discharge is found to be peaked despite the fact that the fueling is from the edge for both the L-mode and the supershot discharges. The intrinsic carbon impurity profile in the supershot discharges is also peaked. This data suggests that the He flux should be described by both a diffusive and convective flux since the source term on axis is negligible Assuming that $\Gamma_{He} = - D_{He}\nabla n_{He} + v_{He}n_{He}$, then both D_{He} and v_{He} increase with minor radius. The resulting value of v_{He} is significantly larger than the predicted neoclassical value and $D_{He} \sim \chi_i^{eff}$. Similar results have been obtained in iron impurity injection experiments. The difference in transport between the electrons and impurities is qualitatively consistent with detailed computations of toroidal drift microinstabilities of the type described by Rewoldt and Tang (1990). In this quasi-linear analysis, electrostatic fluctuations are primarily driven by the spatial gradients of the electrons and ions. These fluctuations in turn account for the transport of the impurity ions. Initial calculations indicate that if the calculated value Γ_{He} were fit to a form of $-D_{He} \nabla n_{He} + v_{He} n_{He}$, then a significant value of the inward pinch would result.

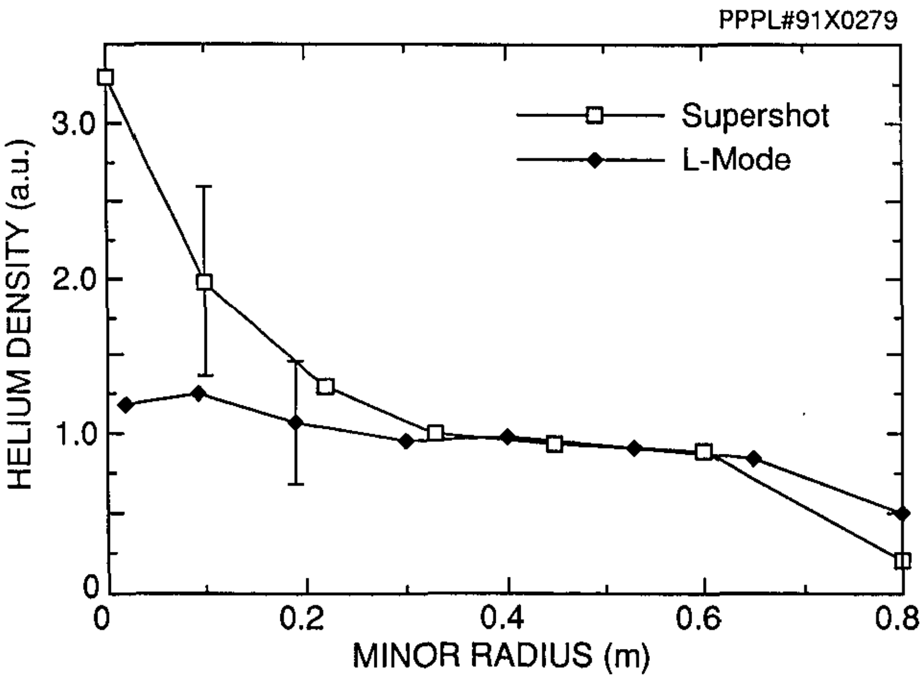

Fig. 9 Comparison of quasistationary He profiles in L-mode and supershot discharges 150ms after a short He puff. The profiles are normalized to each other at r = 0.4m. For both discharges R_p = 2.45m, I_p = 1.0MA, P_{NBI} = 13MW.

The previous discussion suggests that the simple model of transport driven by electrostatic drift instabilities could account for the experimentally observed trends. However, the use of such simple analysis estimates cannot be universally justified because the observed experimental values can vary over a large range in collisionality, density scale length, and β among other parameters of importance. In supershot discharges, $\chi_i^{eff}(r = a/3)$ is found to decrease with increasing temperature as the density scale length decreases from that in L-mode discharges. This is in marked contrast with the results found in L-mode discharges: here both D^{eff} and χ_i^{eff} increase with increasing temperature. These trends are shown in Fig. 10. For comparison, the upper bound on the transport of fast ions is shown. Using the same kinetic stability code described earlier, Tang and Rewoldt (1991) have calculated the temperature variation of the diffusivity in L-mode discharges with broad density profiles and in supershot discharges with peaked density profiles. These initial results are encouraging in that they indicate the expected unfavorable ion temperature dependence in L-mode but a weak (though not favorable) dependence in supershot discharges. The well known difficulties with electrostatic models are the variation with minor radius and the scalings with density, toroidal field, plasma current and ion mass. While experimentally the thermal diffusivity increases significantly with minor radius, the electrostatic models predict that it should decrease with radius, particularly over the outer half of the plasma. Recent density scans in ICH and beam-heated L-mode discharges at fixed power and current are not consistent with a simple analytic relationship of the form $\chi^{eff} \propto T_e^{(1.5-2.5)}/(L_{ne}^2 n_e)$ or $T_e^{(1.5-2.5)}/(L_{ne}L_{Te}n_e)$ where we define $\chi^{eff} \equiv -(q_i + q_e)/(n_i\nabla T_i + n_e\nabla T_e)$. The thermal stored energy at fixed power scales weakly with $\bar{n}_e$ which is inconsistent with $\chi^{eff} \propto T_e^2$ since $T_e(0)$ is nearly inversely proportional to the density. *Detailed analysis of these density scans will provide another test of the* kinetic stability code in the near future.

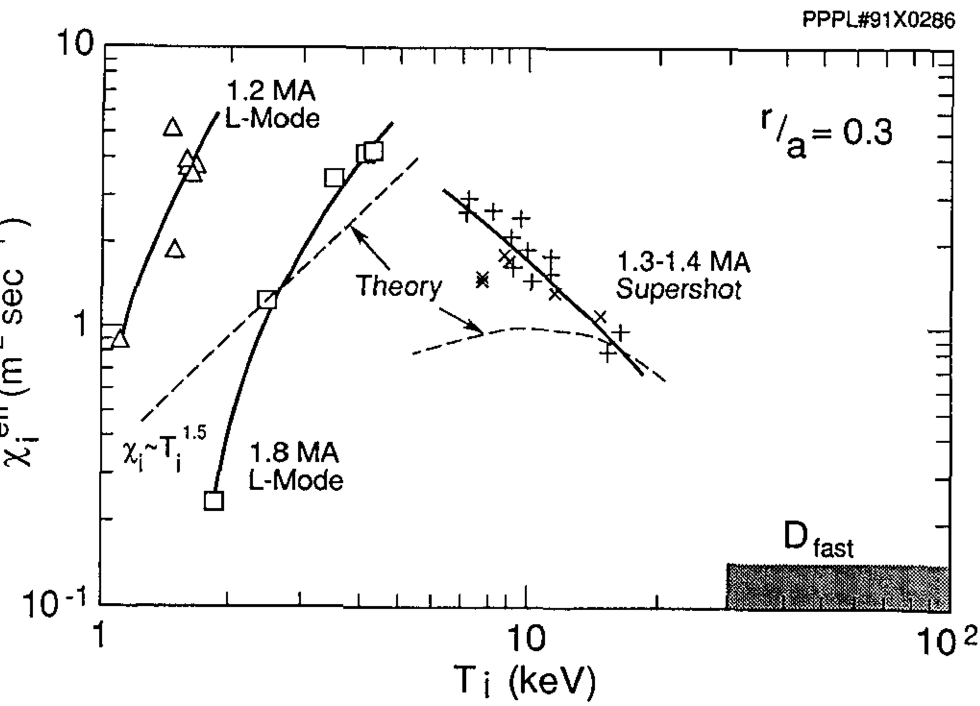

Fig. 10 χ_i^{eff} versus ion temperature for L-mode and supershot discharges compared with the theoretical predictions of Tang and Rewoldt (1991). The upper bound for the *diffusivity of fast ions, discussed in Sec. III, is* also shown.

The observation of enhanced confinement in experiments with peaked density profiles (pellet-fueled, IOC, counter neutral beam injection on ASDEX, supershots, and the JET PEP mode) and the improvement of confinement in the ion channel has focused attention on the role of ion temperature gradient driven turbulence (ITGDT). (See Stambaugh *et al.*, 1990 for a review of work in this area.) This was reinforced by the work of Zarnstorff *et al.* (1989b) who observed that in TFTR supershots in steady-state $\eta_i \approx \eta_i^c$ as predicted by Romanelli (1989) and Hahm and Tang (1989), although the predicted radial profile and magnitude of χ_i for ITGDT were found to be in disagreement with experimental measurement in L-mode discharges. This motivated a series of experiments (Zarnstorff *et al.* 1990b, 1990c; Efthimion *et al.* 1991) in which a supershot target, where initially $\eta_i \approx \eta_i^c$, was perturbed by the injection of either carbon or deuterium pellets or by a short burst of gas such that η_i became transiently much larger than η_i^c. As a result of the perturbation, L_{ne} increased by a factor of ~8 and the T_i profile became slightly steeper (L_{Ti} decreased). What was expected was a dramatic increase in the value of χ_i, that would force the profiles back to "marginal stability" ($\eta_i \approx \eta_i^c$), since the predicted value for the ion heat transport was much larger than observed. The analysis by Zarnstorff *et al.* (1990b) using TRANSP indicates that χ_i^{eff} was not changed by the perturbation. Analytic fluid-type calculations of χ_i for the fully turbulent ITGDT transport (Biglari *et al.*, 1990) are a factor of 3 to 30 greater than observed implying that marginal stability should be enforced. However, kinetic quasi-linear numerical calculations (Rewoldt and Tang, 1990) in toroidal geometry of drift-modes driven by both ion temperature gradients and electron dynamics indicate that the total transport associated with the most unstable modes should be approximately unchanged by the perturbation and that the transport is much lower than the fluid predictions. These results suggest that nonlinear fluid theories of ITGDT transport might be brought into agreement with the experiment by a better treatment of toroidal and kinetic effects. In any case, further work is required to develop a reliable predictive capability for the observed transport.

Empirical global scaling relationships fit a broad range of experimental (L-mode) conditions from various machines reasonably well. However, a similar unifying relationship for the local diffusivity has not been achieved. As discussed above, this may be a consequence of the transport fluxes being highly nonlinear or perhaps being enforced by a marginal stability requirement. Another possibility is that the transport is non-local, meaning that the local transport coefficients are determined not by local quantities (such as v^*, β, L_{ne} or L_{Ti} etc.) but by the value of such quantities elsewhere within the discharge. One example of non-local phenomena is the profile redistribution associated with the sawtooth instability. The possibility that non-local transport may play a role in the quiescent region of a discharge has been raised by an old result and has been brought to attention by several recent experiments as well. Previously, Fredrickson *et al.* (1987) and Taylor *et al.* (1989) reported that the electron temperature scale length is a weak function of heating profiles and, outside the q = 1 surface is a weak function of q. This concept of "profile consistency" (or rather "profile resiliency", which recognizes the fact that the profiles are not rigidly constant) provides a good description of the electron temperature profile. In L-mode discharges, Scott *et al.* (1990c) observed that χ_e^{eff} and χ_i^{eff} decreased everywhere when the plasma current was increased. This is surprising because the calculated current density in the core does not change appreciably as the plasma current is increased due to the sawteeth phenomena. One might, therefore, have expected the change to be predominantly in the outer half of the plasma where the change in the current density, or q profile, is greatest.

The above results, together with the theoretical problem that electrostatic drift wave models do not predict the observed current scaling, motivated an experiment by

Zarnstorff *et al.* (1990b) to perturb the current profiles locally and to evaluate how the local transport evolved. Plasmas in approximate steady-state were contrasted with cases where I_p was rapidly changed from 2MA to 1MA or vice-versa during 2 seconds of balanced neutral-beam heating, as shown in Fig. 11. During the steady state and I_p ramp-down conditions, the line-average density, $\bar{n}_e$, was maintained at a constant value by gas puffing. The rapid change in I_p produces large transient variations of the inferred $j_{\parallel}$ and q profiles as demonstrated by the change in the calculated internal inductance ℓ_i. The energy confinement times, τ_E, of the constant-current plasmas are in good agreement with L-mode scaling. Following the current rampdown or rampup, the energy confinement time does not follow the L-mode relationship ($\tau_E^L \propto I_p$), but relaxes towards it only on a time-scale comparable to the resistive equilibration time, which is several seconds for the case shown, much longer than the energy confinement time itself. Since B_p and q near the edge of the plasma depend on I_p and not (to lowest order) on the current profile, this indicates that I_p scaling is not due to a direct dependence on the edge value of these quantities.

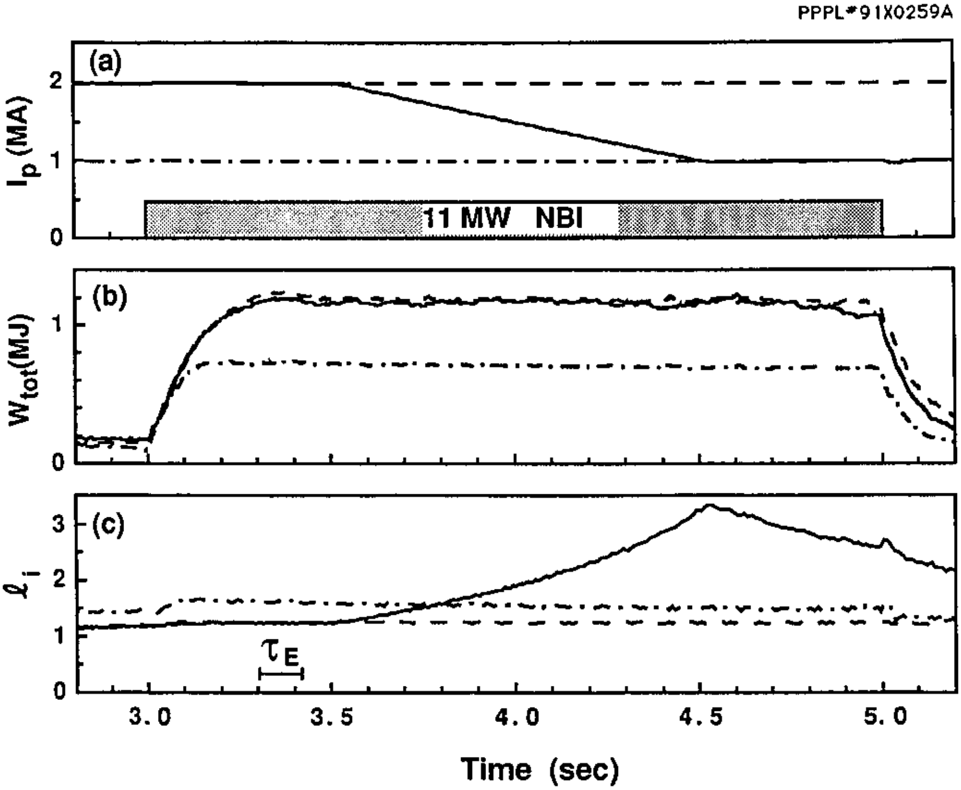

Fig. 11 Time evolution of (a) I_p, (b) W_{tot} measured by the diamagnetic loop, (c) l_i from TRANSP modelling for deuterium plasmas with I_p = 1 MA, I_p = 2 MA and I_p decreased from 2 to 1 MA. For these plasmas B_t = 4.8T, R = 2.45m, a = 0.8m and $\bar{n}_e$ = 3.4 × 10^{19}m^{-3}.

The evolution of the current profile in these plasmas has been calculated by TRANSP. The calculations indicate that a skin current penetrates to ~ a/2 (for the plasma shown) during the available beam-heating pulse. This is confirmed by the observed evolution of the sawtooth inversion radius, indicative of the $q = 1$ radius, which is just beginning to change at the end of the beam-heating pulse. The changes in the q profile are calculated to transiently increase (decrease) the shear $\hat{s} = (r/q)\partial q/\partial r$ by a factor of ~2 during the I_p decrease (increase) sequence. During the change in I_p and the resistive penetration of the current perturbation, the measured T_e, T_i, and n_e profiles are not affected until the current perturbation reaches the plasma core ($r/a < 0.5$). As a consequence, the experimentally inferred χ_e^{eff} do not change, implying that the transport in the outer region ($r > a/2$) cannot depend strongly on the local $j_\parallel$, q, or $\hat{s}$. In particular, these observations imply that, as presently understood, transport due to resistive ballooning modes (Carreras and Diamond, 1989) (which varies as $\sim q^{8/3}/\hat{s}$), neoclassical pressure-gradient turbulence (Kwon, Diamond, and Biglari 1990) (which varies as $\sim q^{7/3}/\hat{s}$), or the Rebut-Lallia model (Rebut et al., 1989) (which varies as $(\nabla T_e - C)q/\hat{s}$ with C varying as $j_\parallel{}^{1/2}/q$), cannot be significant in these plasmas in this region. These observations indicate that L-mode I_p scaling is due to the current profile in the core of the plasma, perhaps near the q = 1 surface. Thus, the observed steady-state dependence of χ_e^{eff} on I_p across the entire profile must be due either to an additional parameter, correlated with I_p in steady state, or a non-local transport dependence on the current profile, perhaps due to a global instability or radial turbulence propagation. In addition, they indicate that confinement can be substantially enhanced (or degraded) relative to L-mode scaling for a fixed I_p value by modifying the current profile.

VI. NONDIMENSIONAL SCALING EXPERIMENTS

Scaling studies cast in the form of nondimensional parameters not only offer the promise of providing a more physics-based approach to extrapolating to a future device, but may provide insight into the nature of the turbulence responsible for the transport. General considerations developed by Kadomtsev (1975) imply that global confinement should vary according to: $\Omega_i\tau_E = F(\rho^*, \nu^*, \beta, Z_{eff}, q, ...)$ where Ω_i is the ion gyro frequency and F is a function of averages over the profile of "nondimensional" quantities. Perkins (1990) has identified 19 nondimensional parameters which could potentially influence transport. On TFTR, scans in which all but one of these nondimensional quantities were held constant were performed (Waltz et al. 1990a). Scans in the normalized gyroradius, $\rho^* = \rho_s/a = (2T_e(0)m_i)^{1/2}/eBa$ for reactor typical values of q, β, and ν^* - but not ρ^* itself - have been performed and are of particular interest for extrapolating to future devices. Theories which involve fine-scale turbulence with respect to ρ^* would be expected to follow gyro-reduced Bohm scaling: $\chi_{gB} \propto (\rho_s^2\ \Omega_i)(\rho_s/L)F_{gB}$ where F_{gB} is a function of dimensionless parameters and L is a local scale length. Transport due to long wavelength turbulence with respect to the device size would be Bohm-like with: $\chi_B \propto (\rho_s^2\ \Omega_i)F_B$.

Comparing confinement in discharges which have q, β and ν^* the same while varying the normalized gyroradius, ρ^*, requires that the following conditions be met in a B_T scan at fixed plasma size: $n \propto B^{4/3}$ and $T \propto B^{2/3}$. Then ρ^* varies as $B^{-2/3}$. In such a scan, gyro-reduced Bohm scaling predicts $\tau_E \propto B$ whereas Bohm scaling predicts $\tau_E \propto B^{1/3}$. The experimental challenge in these experiments is to obtain the plasma conditions which maintain all other relevant dimensionless parameters constant.

Two different ρ^* scans have been performed on TFTR, at a low and a high value of the normalized density $n_e/B_T{}^{4/3}$. In addition, scan in ν^* have been performed. In the ρ^* scans, as B_T and n_e were increased, the power necessary to maintain the temperature at $T \propto B_T{}^{2/3}$ scaled approximately as $B_T{}^2$. Within each scan, the global confinement was unchanged, consistent with L-mode scaling and closer to Bohm than gyro-Bohm predictions. Experiments on DIII-D have shown similar results for global confinement but the local diffusivity in those experiments showed a B_T scaling closer to gyro-Bohm (Waltz *et al.*, 1990b). The most recent DIII-D experiments indicate that the local thermal diffusivity could be represented by either Bohm and gyro-Bohm scaling (DeBoo *et al.* 1991). In the TFTR ρ^* scans, values of χ^{eff} show no significant scaling with B_T, consistent with the weak scaling predicted by Bohm but inconsistent with gyro-Bohm scaling.

Another way to look at the scaling of local transport, which does not involve taking radial derivatives of experimental data, is to consider the power flow $q_{exp}(r) = Q_i(r) + Q_e(r)$ through a magnetic surface normalized to what one would expect for gyro-Bohm and Bohm scaling when temperature profile shapes do not vary: $q_{exp}/q_{gB} = [(a^2-r^2)/r^3R] \times e^2B^2q_{exp}/32\sqrt{2}\pi^2 nT_e^{5/2}M^{1/2}$ and $q_{exp}/q_B = \rho^*(q_{exp}/q_{gB})$. Here the radial factor in brackets is introduced for convenience to avoid a large range of values in Fig. 12, which shows the normalized power flows of the two predictions for the low and high density ρ^* scan and the ν^* scan. The Bohm-like scaling better describes the observed dependences. The ν^* scan shows the power flow to be independent of collisionality, at least when $\nu^* < 1$. Analysis of the uncertainty in the evaluation of q_{exp}/q_{Bohm} indicates that most of the scatter at $r = 0.5$m could be attributed to the uncertainty in the diagnostic measurements and it is approximately constant with minor radius. In the ρ^* scans, the electron and ion temperature profile shapes were fairly constant; however, in the ν^* scan, though the electron temperature profile shape remained constant, the ion temperature profile shape did vary systematically.

For these L-mode discharges the power flow through the ion channel dominates. This suggests that the electron temperature should be replaced by the ion temperature in the expressions for normalized power flow. When this is done, the Bohm normalization again describes the data better, although there is a somewhat larger scatter in the data. These results suggest that long wavelength turbulence is primarily responsible for cross-field transport in these L-mode plasmas.

VII. TURBULENCE STUDIES

The inference that the transport is due to electrostatic instabilities has motivated the development of diagnostics to study density perturbations. Three principal diagnostics, microwave scattering, beam emission spectroscopy, and microwave reflectometry have been used. The extraordinary mode microwave scattering system (Bretz *et al.*, 1988) is the most established of these techniques. Scattering in all regimes in the plasma interior shows that the fluctuation spectrum is dominated by values of $k_\perp < 4\text{cm}^{-1}$, which are not spatially well resolved by microwave scattering (Peebles *et al.*, 1990). The measured k-spectrum falls approximately as $k_\perp^{-3}$ in ohmic, L-mode and supershot discharges. In ohmic discharges the apparent width of the spectrum in frequency is generally somewhat greater than $\omega_e^* \equiv k_\theta T_e/eB_tL_n$ with a shift, ω_s, always in the electron diamagnetic drift direction. In ohmic discharges, the largest shifts, ω_s/ω_e^* up to 4, have been observed in high density plasmas ($\bar{n}_e > 3 \times 10^{19}\text{m}^{-3}$). In beam-heated discharges, toroidal plasma rotation dominates the form of the frequency spectrum due to the instrumental averaging of the rotation profile over the scattering volume. The estimated magnitude of $\delta n_e/n_e \approx 0.3\%$ at $r/a = 0.3$ is in approximate agreement with the mixing length estimate $1/\langle k_\perp \rangle L$ where $L = \sqrt{L_nL_{Te}}$. This is consistent with theoretical estimates based on collisionless trapped electron mode turbulence. The scattered power at $r/a = 0.3$ for a fixed value of $k_\perp = 4.2\text{cm}^{-1}$ ($k_\perp\rho_s = 0.5$) has been found to increase with neutral beam heating power in L-mode discharges.

The beam emission spectroscopy diagnostic (BES) diagnostic measures plasma density fluctuations by observing the fluorescence emitted from a neutral beam as it impacts the plasma (Paul and Fonck, 1990). The observed light from the D_α transition

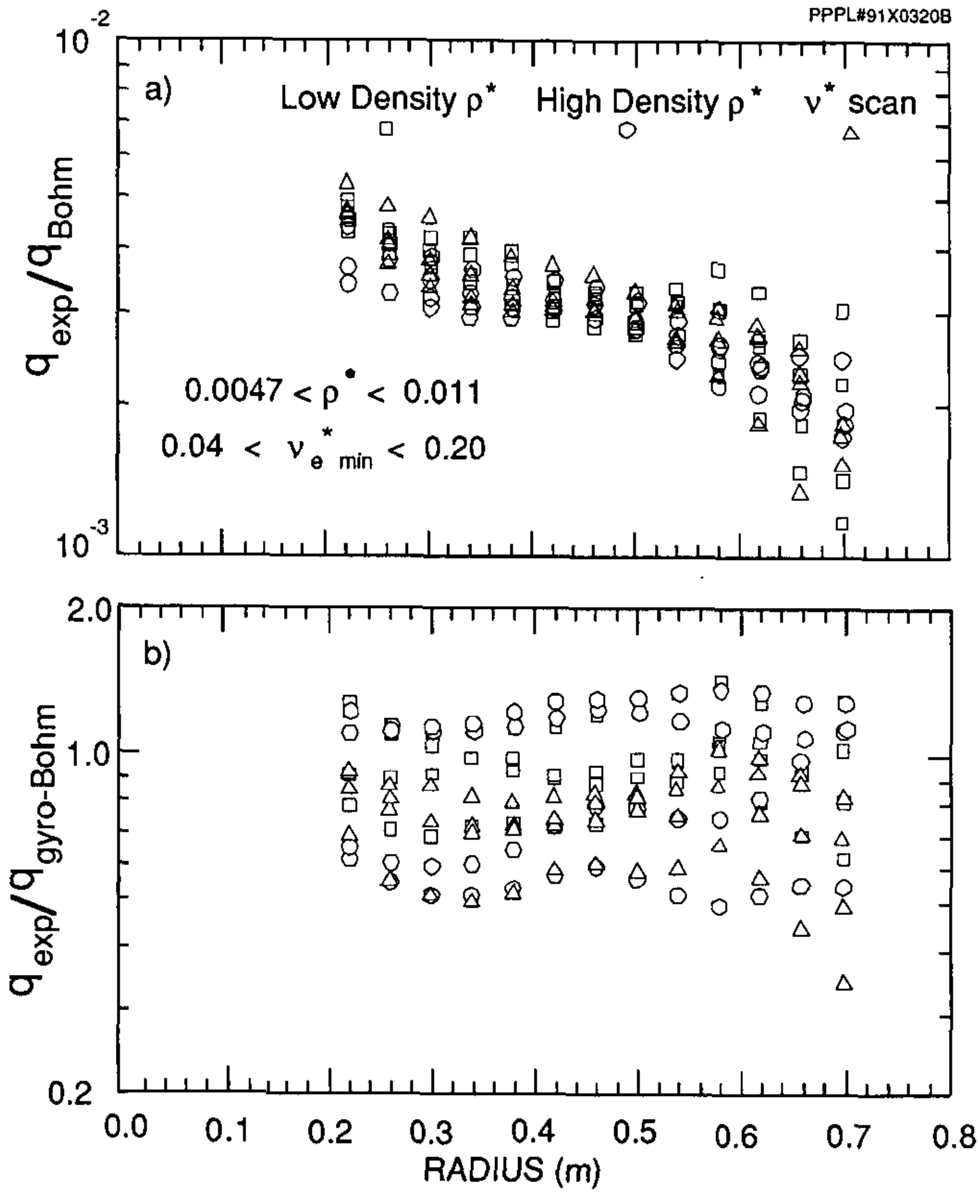

Fig. 12 The radial variation of the total heat flux normalized to the prediction of a) Bohm scaling and b) gyro-reduced Bohm scaling for L-mode plasmas in the high and low density ρ^* scans and the ν^* scan.

($n = 3 \rightarrow 2$), a result of collisional excitation with the plasma ions, is proportional to the fluctuating density. This diagnostic enables the measurement of long wavelength turbulence ($k_\perp < 2\text{cm}^{-1}$) with good spatial resolution (<2cm). Recent results are presented at this meeting by Fonck *et al.* (1991) on L-mode discharges. In the edge region, the density perturbations are large ($\tilde{n}/n \sim 10\%$) and decrease to $\lesssim 1\%$ for $0.5 < r/a < 0.9$. The radial and poloidal correlation lengths decrease with minor radius from values of about 10cm at $r/a = 0.5$ to 2cm at $r/a = 1$.

Furthermore, as shown in Fig. 13, during a power scan in L-mode discharges, the density fluctuation amplitude at $r/a \approx 0.7$ is found to be inversely correlated with the energy confinement time whereas no variation in $\delta n/n$ with τ_E is observed at the edge ($r/a > 0.95$). This data indicates the existence of large-scale fluctuations correlated with enhanced transport. Such fluctuations are poorly resolved spatially by microwave scattering techniques. Trapped-ion modes (Diamond and Biglari, 1990; Biglari and Diamond 1991, and references therein) are theoretically predicted to have these characteristics. Further microinstability calculations, which take into account long radial wavelength properties in toroidal geometry (Marchand *et al.*, 1980), will be performed.

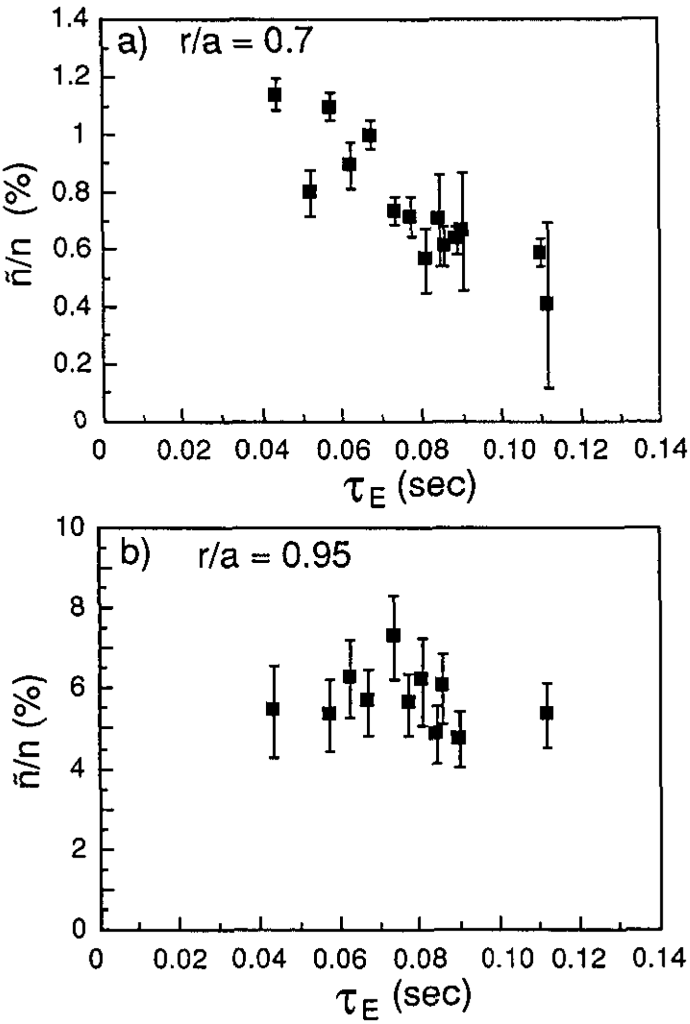

Fig. 13 Amplitude of local density fluctuations in L-mode discharges versus total confinement time for a) an interior region of the plasma and b) the plasma edge.

To extend fluctuation studies to longer wavelengths, a single channel extraordinary-mode 140GHz reflectometer was installed at the end of the last operating period and is now being upgraded to four channels. Initial results in ohmic discharges indicate that fluctuation levels in the plasma core for $k_\perp < 1\mathrm{cm}^{-1}$ are very small,

$\tilde{n}/n < 10^{-4}$, and increase monotonically with minor radius to values of approximately 10^{-2} at the edge of the plasma. Edge density fluctuations with $k_\perp \sim 1cm^{-1}$ and $\tilde{n}/n$ up to 10% have also been observed near the inner wall using visible imaging of ambient H_α light (Zweben and Medley, 1989).

These initial results indicate that in ohmic discharges a peak in the fluctuation spectrum may exist between $1 < k_\perp < 4cm^{-1}$. Experiments with the full complement of reflectometry channels will be performed to complete the study of the k-spectrum and perform a comparison of the results of the different diagnostics in different operating regimes.

VIII. ROLE OF MHD IN TRANSPORT

MHD activity plays an important role in determining plasma performance. For example, performance of supershot discharges is found to be correlated with the stabilization of the sawtooth instability and avoidance of low m/n activity. Discharges with the highest values of density profile peakedness have the longest confinement times and are observed to be sawtooth stabilized. The beam power required to stabilize the sawtooth instability increases with decreasing q(a) (Manickam *et al.*, 1989). The confinement of high current (>2MA) discharges has been, thus far, impaired by the onset of sawteeth. ICH stabilization of sawteeth, which was first demonstrated on JET (Campbell *et al.* 1988), shows great potential for extending the operating regime to higher current (Hosea *et al.*, 1990a, 1990b). Recent experiments at modest powers (P_{NBI} = 11MW and P_{ICH} = 3MW) have demonstrated that it is possible to obtain supershot conditions with ICH and to stabilize the sawtooth instability at relatively high current (2MA), as shown in Fig. 14 (Phillips *et al.*, 1991).

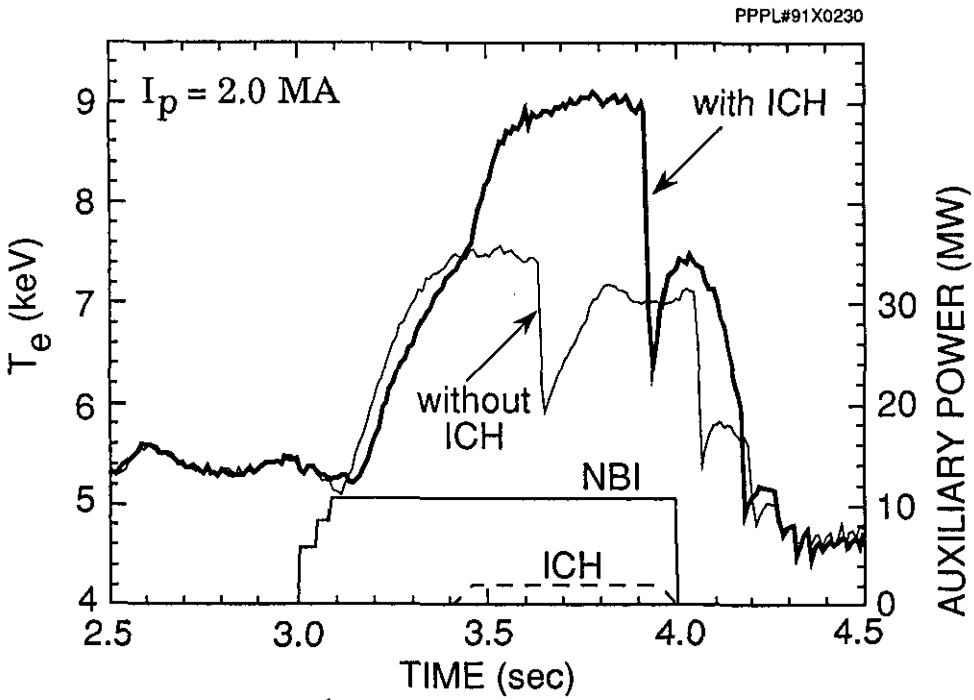

Fig. 14 Sawtooth stabilization of a 2.0MA supershot plasma produced with 11MW of NBI and 3MW of ICH. [R_p = 2.62m, $\bar{n}_e$ = $2.8 \times 10^{19}m^{-3}$, D(^{3}He) regime].

The propagation of heat after the crash phase of the sawtooth instability has been studied by Fredrickson *et al.* (1990) who have modified their previous interpretation (Fredrickson *et al.*, 1986) that the value of heat diffusivity, χ^{HP}, from an analysis of the heat pulse, is larger than that from the power balance, χ^{PB}. The recent analysis shows that the temperature increases beyond the mixing radius after the sawtooth crash. This initial ballistic response has been modeled by a large transient increase in the heat diffusivity. The subsequent propagation of the heat pulse after this redistribution is found to be in reasonable accord with a model that assumes $\chi^{HP} \approx \chi^{PB}$. Whether the increase in the heat diffusivity accompanying the sawtooth crash is due to magnetic stochasticity or due to an increased level of drift wave turbulence remains to be resolved. Nazikian *et al.* (1991) have observed short wavelength, high frequency ($\sim\omega_*$) turbulence in the region of the X-point of the m = 1 island during the sawtooth crash.

Far more deleterious than sawtooth activity is the onset of low-m modes which have set the operational boundaries of the supershot regime $\beta_n \equiv (\beta/(I_p/aB_T) < 2.7$ (%mT/MA) and $\varepsilon\beta_p < 0.7$ (McGuire *et al.*, 1987; Bell *et al.*, 1989). These instabilities can result in either a soft β-collapse ($n \geq 1$) or (less frequently) a rapid disruption ($n = 1$). In recent experiments (Navratil *et al.*, 1990; Sabbagh *et al.*, 1990 and 1991) the current was ramped down just prior to neutral beam injection which significantly increased ℓ_i during the heating. This appeared to suppress the deleterious MHD activity and substantially extended the TFTR limits in both β_n and $\varepsilon\beta_p$ at low plasma current. As shown in Fig. 15, $\varepsilon\beta_p$ was increased to 1.6 and β_n to 4.7. In the discharges with large values of $\varepsilon\beta_p$, a natural inboard poloidal

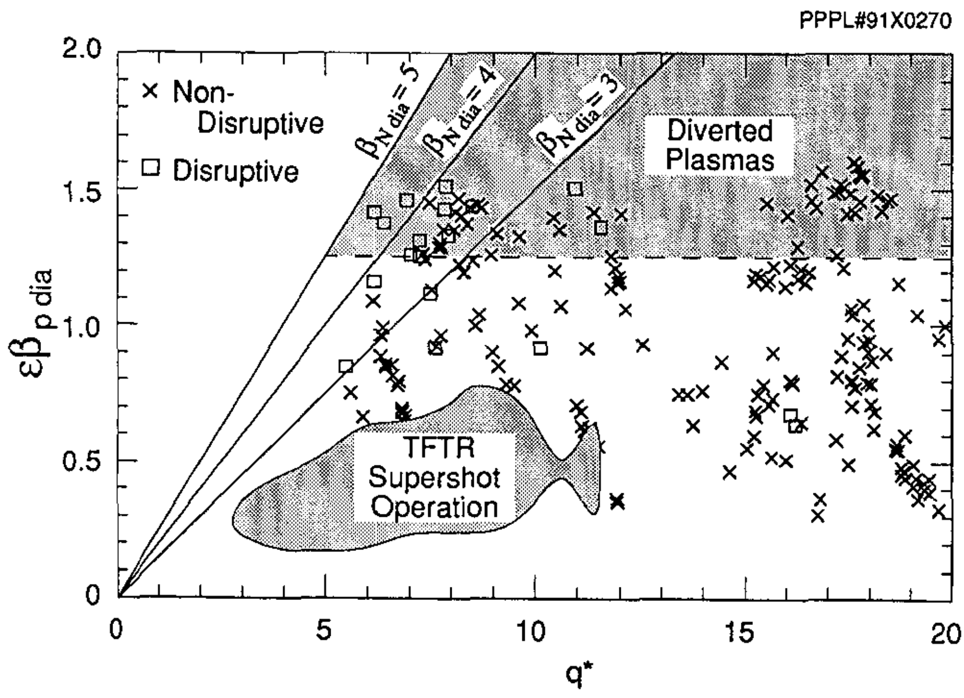

Fig. 15 Summary of $\varepsilon\beta_p$ and β_n in TFTR measured by the diamagnetic loop as a function of $q^* = (5a^2B_t/RI_p(MA)) \times [1 + \kappa^2]/2$ where κ is the plasma elongation. Contours of constant β_n appears as straight lines as shown.

divertor appeared. These discharges have enhanced confinement with $\tau_E/\tau_E^L \le 3$. This enhancement tends to increase as $\varepsilon\beta_p$ increases. Discharges in which the plasma current is ramped down have the largest improvement over L-mode. This operating regime demonstrates that peaking the current profile can both increase the energy confinement time and extend the tokamak operating regime.

In addition to affecting the confinement of the background plasma, MHD instabilities can interact with the fast ions. Zweben *et al.* (1990) have observed that the fusion products are expelled from the plasma when large amplitude low-m instabilities are present and during the crash of the sawtooth. This MHD activity does not appear to be driven by the fast particles. However, since collective interactions driven by fast particles, such as the fishbone instability, have been observed frequently on smaller devices, there are concerns that during deuterium-tritium operation, alpha particles could collectively interact with MHD modes. An instability with a very low predicted threshold (Cheng *et al.*, 1990) is the toroidal Alfvén eigenmode which can be destabilized by the alpha particles with parallel velocity $V_\alpha \sim V_A$. Wong *et al.* (1991a; 1991b) have recently performed a simulation experiment using neutral beams which is reported at this conference. At low toroidal field (~1T) and (relatively) high density ($\bar{n}_e = 2.5 \times 10^{19} m^{-3}$) the theoretical condition for instability $V_b \sim V_A$ can be satisfied. Bursts of MHD activity in the frequency range of the toroidal Alfvén eigenmode were observed when the plasma density was sufficiently high that $V_b/V_A > 0.7$. The observed frequency scaled as the theoretical frequency when varied over a factor of two by varying the plasma density

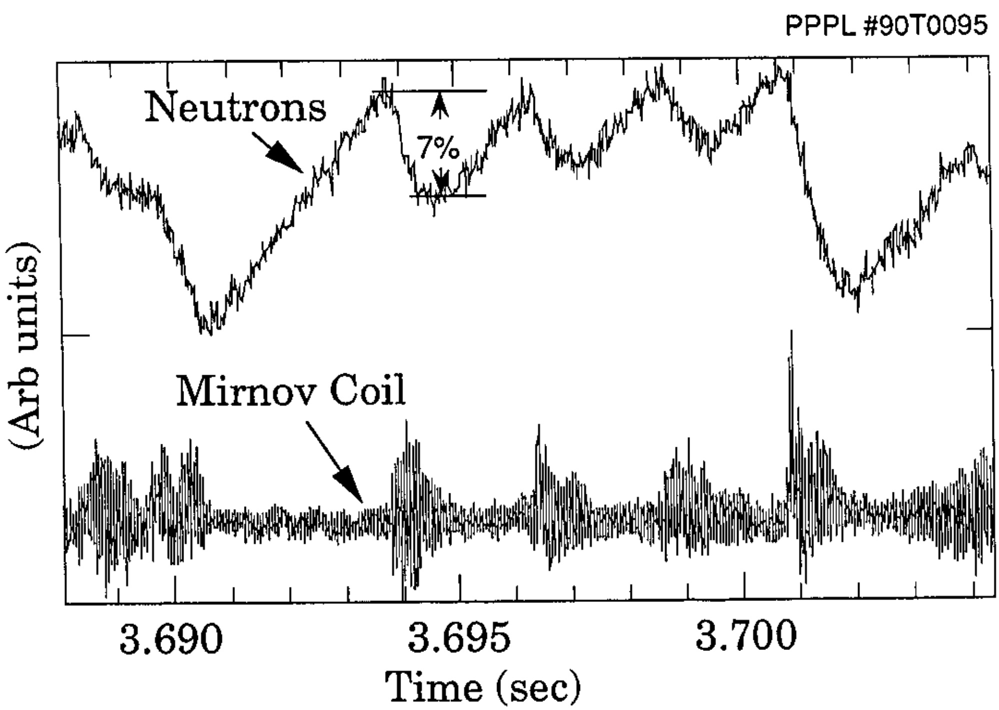

Fig. 16 Correlation between total neutron emission rate and Mirnov coil signal during injection of an energetic (100keV) neutral beam into a relatively high-density ($\bar{n}_e = 2 \times 10^{19} m^{-3}$) plasma at low toroidal field (B_T = 1T). The vertical scale for each trace is linear with a suppressed zero.

and the toroidal field. Beam emission spectroscopy was used to measure the mode structure of the instability inside the plasma ($a/2 < r < a$) which was found to be as expected for a global eigenmode. These experiments also showed a decrease in neutron flux with the occurrence of the MHD fluctuation, indicating the loss of fast beam ions from the plasma, as shown in Fig. 16. Initial estimates indicate that the instability threshold is substantially higher than the theoretically predicted threshold; however, further theoretical work is in progress (Berk *et al.* 1991).

IX. WALL CONDITIONING

Wall conditioning techniques have been and continue to be a key element in the development of the enhanced confinement regime in TFTR. Ohmic He conditioning shots (Dylla *et al.*, 1987) continue to be used to maintain low recycling of the hydrogenic species. Once the hydrogen recycling has been reduced, plasma performance becomes well correlated with the level of CII impurity light from the target plasma. Previous problems with carbon blooms during high-power supershots have been remedied by replacing the graphite tiles in the high heat flux region of the toroidal limiter with carbon-carbon composite tiles which have much higher thermal stress capability (Ulrickson *et al.* 1989, 1990). Further reductions in the influx of carbon were achieved during the 1990 run by injecting lithium pellets prior to beam injection. Snipes *et al.* (1991) at this conference describe the use of pellets to coat the walls with lithium. The result of the lithium injection is to decrease the recycling of carbon and deuterium leading to appreciable, and reliable, increases in the central ion temperature, total plasma stored energy, and peak neutron rate. Using this technique, the maximum neutron source strength of 5×10^{16} neutrons per second, corresponding to a D-D fusion power of 58kW, was achieved with 33MW of heating power. In this discharge, the value of $Q_{DD} = 1.8 \times 10^{-3}$ was among the highest achieved on TFTR. Transport analysis indicates that the improvement with Li pellet injection is mainly due to a reduction in the ion thermal diffusivity by 30 - 60% in the off-axis region $0.25 < r/a < 0.5$. How a relatively minor change to the plasma boundary condition results in a significant change to the core transport coefficients remains a major unanswered question.

X. SUMMARY

Transport studies in L-mode, supershots and H-mode suggest that in discharges without observable MHD activity, the underlying transport is caused by electrostatic turbulence. The relationship between χ_ϕ^{eff}, χ_i^{eff}, χ_e^{eff} and the particle diffusivities and the limits placed on the convection multiplier indicate that strong magnetic stochasticity does not govern transport. The experimental results also indicate that existing theoretical models need to be further developed. The observation of long-scale-length fluctuations being correlated with confinement has significant physical ramifications. Further studies with additional diagnostics over a broader parameter range during the next run will be conducted to explore these thought-provoking results further. The nondimensional scaling experiments indicate that Bohm-like scaling is a better description of the heat flux than gyro-reduced Bohm scaling. This study also implies that long wavelength modes may account for the major part of the observed transport. The current perturbation experiments have shown that I_p scaling is not due to local changes in the q or $\hat{s}$ profile, implying that transport is non-local or that other parameters are subtly correlated and not controlled. Present resistive ballooning models as well as the Rebut-Lallia model do not describe these results. These experiments also indicate that confinement can be controlled through the central current profile. Marginal stability imposed by fluid models of ITGDT has been tested by perturbation experiments which have demonstrated that a large increase in the ion heat diffusivity does not occur when the criteria for the onset of ITGDT are exceeded. These results indicate the need to include kinetic and toroidal effects in the analysis. Although the transport studies have not yet succeeded in developing a reliable theoretically-based predictive capability, they have significantly constrained the theoretical models.

The transport studies have stimulated the development of new operating regimes such as the high-β_p regime, and have demonstrated the importance of current profile control in the next generation of machines. As always, there continues to be an important role for exploration. The development of new wall coating techniques using lithium pellet injection has resulted in extension of the parameter range for neutron source strength and for Q_{DD} in preparation for D-T experiments on TFTR.

Preparations are actively underway to begin D-T operations in 1993. Those experiments will be the natural consequence of the transport studies described here, for not only will they build on these experiments, but they will also enable transport to be investigated in a new regime. For example, the simulation experiments with neutral beam injection of the toroidal Alfvén eigenmode showed that the interaction of MHD and fast ions can be an important process. When extrapolated to D-T, the experimental conditions achieved to date in TFTR will enable the direct study of collectively driven alpha instabilities (Budny *et al.*, 1991). These instabilities could be important in the next generation of machines, BPX and ITER, and will be studied on TFTR.

Acknowledgements

It is a pleasure to acknowledge the contribution of the many engineers and technicians whose efforts and personal sacrifices have enabled us to conduct the experiments described here, to J. D. Strachan for his many contributions, and to J. D. Callen and P. H. Diamond for many stimulating discussions.

REFERENCES

Bell, M. G. *et al.* (1989). Plasma Phys. Control. Nucl. Fus. Res., Proceedings of the Twelfth International Conference, Nice, 1988 (IAEA, Vienna) Vol. I, p. 27.
Berk, H. *et al.* (1991). At this conference.
Biglari, H., Diamond, P. H., and Rosenbluth, M. N. (1989). Phys. Fluids B 1, 109.
Biglari, H., and Diamond, P. H. (1991) To be published in Phys. Fluids B.
Biglari, H. and Chen L. (1991). Submitted to Phys. Fluids.
Bretz, N. *et al.* (1988). Rev. Sci. Instruments 59, 1538.
Boivin, R. L. *et al* (1991). At this conference.
Boozer, A. H. *et al.* (1990). Phys. Fluids B 2, 2870.
Budny, R, *et al.* (1991). At this conference.
Burrell, K. H. *et al.* (1990). Phys. Fluids B 2, 2904.
Bush, C. E. *et al.* (1990). Phys. Rev. Lett. 65, 424.
Callen, J. D. (1990). Phys. Fluids B 2, 2869.
Campbell, D. J. *et al.* (1988). PHys. Rev. Lett. 60, 2148.
Carreras, B.A. and Diamond, P.H. (1989). Phys. Fluid B 1, 1011.
Cheng, C. Z. (1990). Princeton Plasma Physics Laboratory Report PPPL-2717 (Oct. 1990). To be published in Phys. Fluids B.
DeBoo, J. *et al.* (1991). At this conference.
Diamond, P. H., and Biglari, H. (1990). Phys. Rev. Lett. 65, 2865.
Dylla, H. F. *et al.* (1987). Nucl. Fusion 27, 1221.
Efthimion, P. C. *et al.* (1989). Plasma Phys. Control. Nucl. Fus. Res., Proceedings of the Twelfth International Conf., Nice, 1988 (IAEA, Vienna) Vol. I, p. 307.
Efthimion, P. C. *et al.* (1991a). Phys. Rev. Lett. 28, 421.
Efthimion, P. C. *et al.* (1991b). To be published in Phys. Fluids B.
Fredrickson, E. D. *et al.* (1986). Nucl. Fusion 26, 849.
Fredrickson, E. D. *et al.* (1987). Nucl. Fusion 27, 1897.
Fredrickson, E. D. *et al.* (1990). Phys. Rev. Lett. 65, 2869
Fonck, R. J. *et al.* (1989). Phys. Rev. Lett. 63, 520.

Fonck, R. J. *et al.* (1991). At this conference.
Goldston, R. J. *et al.* (1981). J. Comput. Phys. 43, 61.
Goldston, R. J. *et al.* (1984). Plasma Phys. Control. Fusion 26, 87.
Goldston, R. J., White, R., and Boozer, A. (1981). Phys. Rev. Lett. 47, 647.
Grisham, L. R. *et al.* (1990). Controlled Fusion and Plasma Heating, Proceedings of the Seventeenth European Conference, Amsterdam, 1990, Vol. 14B, Part I, p. 146.
Grisham, L. R. *et al.* (1991). Submitted for publication in Phys. Rev. Lett.
Groebner, R. J. *et al.* (1985). Nucl. Fusion 26, 543.
Hahm, T. S. and Tang, W. M. (1989). Phys. Fluids B 1, 1185.
Hammett, G. (1986). Ph.D. Thesis, Princeton University (1986). Available from University Microfilm, Ann Arbor, MI 48106 USA.
Hawryluk, R. J. (1980). In Coppi, B. *et al.*, editors, Physics of Plasmas Close to Thermonuclear Conditions, (CEC, Brussels, 1980) Vol. I, p. 19.
Hawryluk, R. J. *et al.* (1987). Plasma Phys. Control. Nucl. Fus. Res., Proceedings of the Eleventh International Conference, Kyoto, 1986 (IAEA, Vienna) Vol. I, p. 51.
Heidbrink, W. *et al* (1991). In preparation.
Hirshman, S. P., and Sigmar, D. J. (1981). Nucl. Fusion 21, 1079.
Hosea, J. C. *et al.* (1990a). Proceedings of the Joint Varenna-Lausanne International Workshop on Theory of Fusion Plasmas, August 1990.
Hosea, J. C. *et al.* (1990b). Proceedings of the Thirteenth International Conference on Plasma Physics and Controlled Nuclear Fusion Research, Washington, 1990 (IAEA, Vienna) Paper IAEA-CN-53/E-1-5 to appear.
Houlberg, W. A. *et al.* (1990). Phys. Fluids B 2, 2913.
Hulse, R. *et al.* (1991). Presented at Transport Task Force Workshop (Austin, TX).
Kadomtsev, B. (1975). Sov. J. Plasma Phys. 1, 295.
Kaye, S. M. *et al.* (1990). Phys. Fluids B 2, 2926.
Kwon, O. J., Diamond, P. L., and Biglari, H. (1990). Phys. Fluid B 2, 291.
Manickam, J. *et al.* (1989). Plasma Phys. and Control. Nucl. Fus. Res., Proceedings of the Twelfth International Conference, Nice, 1988, (IAEA, Vienna) Vol. I, p. 395.
Marchand, R., Tang, W. M., and Rewoldt, G. (1980). Phys. Fluids 23, 1164.
Meade, D. M. *et al.* (1990). Proceedings of the Thirteenth International Conference on Plasma Physics and Controlled Nuclear Fusion Research, Washington, 1990 (Vienna) Paper IAEA-CN-53/A-1-1, to appear.
McGuire, K. *et al.* (1987). Plasma Phys. Control. Nucl. Fus. Res., Proceedings of the Eleventh International Conference, Kyoto, 1986 (IAEA, Vienna) Vol. I, p. 421.
Mynick, H. E., and Duvall, R. E. (1989). Phys. Fluids B 1, 750.
Navratil, G. A. *et al.* (1990). Proceedings of the Thirteenth International Conference on Plasma Physics and Controlled Nuclear Fusion Research, Washington, 1990 (IAEA, Vienna) Paper IAEA-CN-53/A-3-3, to appear.
Nazikian, R. *et al.* (1991). At this conference.
Paul, S. F., and Fonck, R. J. (1990). Rev. Sci. Instrum. 61, 3496.
Peebles, W. A. *et al.* (1990). Proceedings of the Thirteenth International Conference on Plasma Physics and Controlled Nuclear Fusion Research, Washington, 1990 (IAEA, Vienna) Paper IAEA-CN-53/A-7-1, to appear.
Perkins, F. (1990). Princeton Plasma Physics Lab. Report PPPL-2708.
Phillips, C. K. *et al.* (1991). At this conference.
Radeztsky, R. H. *et al.* (1988). Controlled Fusion and Plasma Heating, Proceedings of the Fifteenth European Conference, Dubrovnik, 1988. Vol. 12B, Part 1, p. 79.
Rebut, P. H., Lallia, P. P., and Watkins, M. L. (1989). Plasma Phys. and Control. Nucl. Fus. Res., Proceedings of the Twelfth International Conference, Nice, 1988 (IAEA, Vienna) Vol. II, p. 191.
Rewoldt, G. and Tang, W.M. (1990). Phys. Fluid B 2, 318.
Romanelli, F. (1989). Phys. Fluid B 1, 1018.
Ross, D. W. *et al.* (1987). IPSG Panel Report No. DOE/ET-53193-7.
Sabbagh, S. A. *et al.* (1990). Controlled Fusion and Plasma Heating, Proceedings of the Seventeenth European Conference, Amsterdam 1990, Vol. 14 B, Part 1, p. 387.
Sabbagh, S. A. *et al.* (1991). To be published in Phys. Fluids B.
Scott, S. D. *et al.* (1987). Controlled Fusion and Plasma Physics, Proceedings of the Fourteenth European Conference, Madrid, 1987, Vol 11D, Part 1, p. 65.
Scott, S. D. *et al* (1989). Plasma Phys. Control. Nucl. Fus. Res., Proceedings of the Twelfth International Conference, Nice, 1988 (IAEA, Vienna) Vol. I, p.655.
Scott, S. *et al* (1990a). Phys. Rev. Lett. 64, 531.
Scott, S. D. *et al.* (1990b). Phys. Fluids B 2, 1300.
Scott, S. D. *et al.* (1990c). Proceedings of the Thirteenth International Conference on Plasma Physics and Controlled Nuclear Fusion Research, Washington, 1990 (IAEA, Vienna) Paper IAEA-CN-53/A-3-6, to appear.
Smithe, D. N., Colestock, P. L.,.Kashuba, R. J., and Kamach, T. (1987). Nucl. Fusion 27, 1319.
Snipes, J. A. *et al.* (1991). At this conference.

Stambaugh, R. D. *et al.* (1990). Phys. Fluids B 2, 2941.
Strachan, J. D. *et al.* (1987). Phys. Rev. Lett. 58, 1004.
Stratton, B. C. *et al.* (1991). Nucl. Fusion 31, 171.
Synakowski, E. J. *et al.* (1990). Phys. Rev. Lett. 65, 2255.
Takase, Y. *et al.* (1991). In preparation.
Tang, W. M. and Rewoldt, G. (1991). Presented at the Sherwood Meeting, Seattle, (April 1991).
Taylor, G. *et al.* (1989). Nucl. Fusion, 29, p. 3.
Ulrickson, M. *et al.* (1989). Plasma Phys. Control. Nucl. Fus. Res., Proceedings of the Twelfth International Conference, Nice, 1988 (IAEA, Vienna) Vol. III, p. 419.
Ulrickson, M. *et al.* (1990). J. Nucl. Mater. 176/177, 44.
Waltz, R. E. *et al.* (1990a). Proceedings of the Thirteenth International Conference on Plasma Physics and Controlled Nuclear Fusion Research, Washington, 1990, (IAEA, Vienna) Paper IAEA-CN-53/D-4-7, to appear.
Waltz, R. E., DeBoo, J. C., and Rosenbluth, M. N. (1990b). Phys. Rev. Lett. 65, 2390.
Wong, K. L. *et al.* (1991a). Phys. Rev. Lett. 66, 1874.
Wong, K. L. *et al.* (1991b). At this conference.
Wootton, A. J. *et al.* (1990). Phys. Fluids B 2, 2879.
Yushmanov, P. *et al.* (1990). Nucl. Fusion 25, 65.
Zarnstorff, M. C. *et al.* (1987). Controlled Fusion and Plasma Physics, Proceedings of the Fourteenth European Conference, Madrid, 1987. Vol. 11D, Part 1, p. 144.
Zarnstorff, M. C. *et al.* (1988a). Phys. Rev. Lett. 60, 1306.
Zarnstorff, M. C. *et al.* (1988b). Controlled Fusion and Plasma Heating, Proceedings of the Fifteenth European Conference, Dubrovnik, 1988. Vol. 12B, Part 1, p. 95.
Zarnstorff, M. C. *et al.* (1989a). Plasma Phys. Control. Nucl. Fus. Res., Proceedings of the Twelfth International Conf., Nice, 1988, (IAEA, Vienna) Vol. I, p. 183.
Zarnstorff, M. C. *et al* (1989b). Controlled Fusion and Plasma Physics, Proceedings of the Sixteenth European Conference, Venice 1989. Vol. 13B, Part 1, p. 35.
Zarnstorff, M. C. *et al.* (1990a). Phys. Fluids B 2, 1852.
Zarnstorff, M. C. *et al.* (1990b). Proceedings of the Thirteenth International Conference on Plasma Physics and Controlled Nuclear Fusion Research, Washington, 1990 (IAEA, Vienna) Paper IAEA-CN-53/A-II-2, to appear.
Zarnstorff, M. C. *et al.* (1990c). Controlled Fusion and Plasma Heating, Proceedings of the Seventeenth European Conference, Amsterdam, 1990. Vol. 14B, Part 1, p. 42.
Zweben, S. J., and Medley, S. S. (1989). Phys. Fluids B 1, 2058.
Zweben, S. J. *et al.* (1990). Nucl. Fusion 30, 1551.
Zweben, S. J. *et al.* (1991). Princeton Plasma Physics Laboratory Report PPPL-2770.